(This is a sample cover image for this issue. The actual cover is not yet available at this time.)

Journal of Theoretical Biology 321 (2013) 8–27

Contents lists available at SciVerse ScienceDirect

Journal of Theoretical Biology

journal homepage: www.elsevier.com/locate/yjtbi

A mathematical model of the human menstrual cycle for the administration of GnRH analogues

Susanna Röblitz [a,c,*], Claudia Stötzel [a,c], Peter Deuflhard [a,b,c], Hannah M. Jones [d], David-Olivier Azulay [e], Piet H. van der Graaf [f], Steven W. Martin [f]

[a] Computational Systems Biology Group, Zuse Institute Berlin (ZIB), Takustraße 7, 14195 Berlin, Germany
[b] Department of Mathematics and Computer Science, Freie Universität Berlin, Arnimallee 6, 14195 Berlin, Germany
[c] DFG Research Center Matheon "Mathematics for Key Technologies", Berlin, Germany
[d] Department of Pharmacokinetics, Dynamics and Metabolism, Pfizer, Ramsgate Road, Sandwich, Kent CT13 9NJ, United Kingdom
[e] Molecular Medicine, Pfizer, Ramsgate Road, Sandwich, Kent CT13 9NJ, United Kingdom
[f] Pharmacometrics, Global Clinical Pharmacology, Pfizer, Ramsgate Road, Sandwich, Kent CT13 9NJ, United Kingdom

HIGHLIGHTS

- Menstrual cycle feedback mechanisms are described using differential equations.
- GnRH, FSH, LH, E2, P4, inhibins A and B, and follicular development are modeled.
- The model predicts hormonal changes following GnRH analogue administration.
- Simulation results agree with measurements of hormone blood concentrations.
- The model gives insight into mechanisms underlying gonadotropin suppression.

ARTICLE INFO

Article history:
Received 2 March 2012
Received in revised form
27 September 2012
Accepted 19 November 2012
Available online 1 December 2012

Keywords:
Endocrinology
Reproduction
Hormone secretion
Systems pharmacology
Periodic behavior

ABSTRACT

The paper presents a differential equation model for the feedback mechanisms between gonadotropin-releasing hormone (GnRH), follicle-stimulating hormone (FSH), luteinizing hormone (LH), development of follicles and corpus luteum, and the production of estradiol (E2), progesterone (P4), inhibin A (IhA), and inhibin B (IhB) during the female menstrual cycle. Compared to earlier human cycle models, there are three important differences: The model presented here (a) does not involve any delay equations, (b) is based on a deterministic modeling of the GnRH pulse pattern, and (c) contains less differential equations and less parameters. These differences allow for a faster simulation and parameter identification. The focus is on modeling GnRH-receptor binding, in particular, by inclusion of a pharmacokinetic/pharmacodynamic (PK/PD) model for a GnRH agonist, Nafarelin, and a GnRH antagonist, Cetrorelix, into the menstrual cycle model. The final mathematical model describes the hormone profiles (LH, FSH, P4, E2) throughout the menstrual cycle of 12 healthy women. It correctly predicts hormonal changes following single and multiple dose administration of Nafarelin or Cetrorelix at different stages in the cycle.

1. Introduction

GnRH plays an important role in the female menstrual cycle (Neill, 2006). It controls the complex process of follicular growth, ovulation, and corpus luteum development. GnRH is responsible for the synthesis and release of the gonadotropins FSH and LH from the anterior pituitary to the blood (Hall, 2009). These processes are controlled by the size and frequency of GnRH pulses. In males, the GnRH pulse frequency is constant, but in females, the frequency varies during the menstrual cycle, with a large surge of GnRH just before ovulation. Low-frequency pulses lead to FSH release, whereas high frequency pulses stimulate LH release (Marshall and Griffin, 1993). Thus, pulsatile GnRH secretion is necessary for correct reproductive function. Since GnRH itself is of limited clinical use due to its short life-span, modifications around its lead structure have led to GnRH *analogues* whose overall aim is to suppress the gonadotropins (Engel and Schally, 2007).

There are two types of GnRH analogues: agonists and antagonists. GnRH *agonists* act just like natural GnRH, resulting in an

* Corresponding author at: Computational Systems Biology Group, Zuse Institute Berlin (ZIB), Takustraße 7, 14195 Berlin, Germany. Tel.: +49 30 84185 156; fax: +49 30 84185 107.
E-mail address: susanna.roeblitz@zib.de (S. Röblitz).

0022-5193/$ - see front matter © 2012 Elsevier Ltd. All rights reserved.
http://dx.doi.org/10.1016/j.jtbi.2012.11.020

initial increase in FSH and LH secretion (“flare effect”). After their initial stimulating action, agonists are able to exert a prolonged suppression effect on the receptors, termed “down-regulation” or “desensitization”, which can be observed after about 10 days (vanLoenen et al., 2002). Usually, this induced and reversible hypogonadism is the therapeutic goal. GnRH agonists are used, for example, for the treatment of cancer, endometriosis, uterine fibroids, and precocious puberty, as well as for in vitro fertilization (IVF) (Engel and Schally, 2007). GnRH *antagonists* compete with natural GnRH for binding to GnRH receptors, but the antagonist–receptor complex has no effect on the gonadotropins. Thus, antagonists lead to an acute suppression of the hypothalamic–pituitary–gonadal (HPG) axis without an initial gonadotropin surge. Today, GnRH antagonists are mainly used in IVF treatment to block natural ovulation (Cetrorelix, Ganorelix) and in the treatment of prostate cancer (Abarelix, Degarelix) (Engel and Schally, 2007). For several reasons, such as high dosage requirements and the incidence of allergies at an early stage of drug development, the commercialization of GnRH antagonists lagged behind their agonist counterparts (Garnick, 2001). Therefore, GnRH agonists became more popular in IVF treatment, even though antagonist treatment is easier to conduct (shorter treatment period, reduced risk for ovarian hyperstimulation syndrome) and reproductive outcomes are comparable (Griesinger and Diedrich, 2007).

The aim of the present paper is to develop a mathematical model that characterizes the actions of GnRH agonists and antagonists by their different effects on the HPG axis. The model should be able to explain blood concentrations of LH, FSH, E2, and P4 after single and multiple dose treatment with a GnRH analogue during different stages of the menstrual cycle, as reported in Duijkers et al. (1998), Leroy et al. (1994), Monroe et al. (1985) and Monroe et al. (1986). Such a model should eventually help in preparing and monitoring clinical trials with new drugs that affect GnRH receptors, as well as in the selection of new targets in this pathway. We thus aim at contributing to the newly emerging discipline of quantitative and systems pharmacology (QSP) (Ward, 2011), which combines systems biology and pharmacology in academia and industry in order to enhance drug discovery and development (van der Graaf, 2012).

Since data are available only for some model features, we follow a semi-mechanistic modeling approach, in which mechanistic aspects of physiologic processes, e.g. feedback loops along the HPG axis, are combined with some heuristic features, e.g. follicular stages of maturation. Hill functions are used to model qualitative features such as inhibitory or stimulatory effects.

Although comprising several organs (hypothalamus, pituitary, blood, ovaries), the model presented here does not take into account signal transduction on a cellular level. Bridging the gap between multiple scales in space and time is definitely a challenging task on the biological modeling agenda. The authors do hope that making our mathematical tools accessible to a general audience will support this process.

Nevertheless, the purpose of the present paper is to provide a starting point for an incremental model development in terms of equations and parameter values for the human menstrual cycle. We hope that other researchers will be enabled to refine the presented model, once new approaches for incorporating processes at several temporal and spatial scales are available.

There already exist PK/PD models for GnRH analogues (Nagaraja et al., 2003; Tornøe et al., 2006; Jadhav et al., 2006). These models describe the influence on LH and/or FSH but do not include GnRH receptor binding mechanisms. Our goal is to merge such a PK/PD model via detailed GnRH receptor binding mechanisms with a large kinetic model of the fully coupled feedback mechanisms in the human menstrual cycle. At present, there are only few publications available that focus on these feedback mechanisms. In 1999, a differential equation model that contains the regulation of LH and FSH synthesis, release, and clearance by E2, P4, and Ih was introduced by Selgrade and Schlosser (1999) and Schlosser and Selgrade (2000). This model was extended by Selgrade (2001), Harris (2001), Harris Clark et al. (2003) and later by Pasteur (2008) to describe the roles of LH and FSH during the development of ovarian follicles and the production of the ovarian hormones E2, P4, IhA, and IhB. Reinecke and Deuflhard (2007) and Reinecke (2009) added, among other things, a stochastic GnRH pulse generator and GnRH receptor binding mechanisms.

Parametrization of the model in Reinecke and Deuflhard (2007) and Reinecke (2009) was based on averaged data for LH, FSH, E2, and P4 throughout one normal cycle. Our first goal was to check whether that model was capable of predicting a situation that had not been used to parametrize it, namely the administration of GnRH analogues. Unfortunately, its predictive capacity turned out to be limited. Simulations of GnRH analogue treatments via the existing GnRH equations were unable to adequately describe the decrease in free GnRH receptors following single agonist doses. Moreover, the menstrual cycle did not return to its initial state at the beginning of the next cycle. In addition, the pulsatile pattern of GnRH required extremely small computational timesteps which led to intolerable simulation times. Simply re-parameterizing the model did not improve the results because mechanistic details essential for our new aims were missing. Hence, re-parametrization had to be accompanied by both model reduction and model refinement to explain the new experimental data from GnRH analogue treatments, while maintaining the fit to former normal cycle data. The results of this intensive collaboration over years are presented here.

The paper is organized as follows. In Section 2 we derive the model equations with special focus on GnRH receptor binding and the coupling to a PK model. Simulation results for the normal cycle as well as for the treatment with Nafarelin and Cetrorelix are presented and discussed in Section 3. The conclusion follows in Section 4. Details on data sources, initial values and parameter values as well as consistency of units are postponed to an appendix.

2. Model equations

A qualitative description of the model to be presented is illustrated as a flowchart in Fig. 1. In the hypothalamus, the hormone GnRH is formed, which reaches the pituitary gland through the portal system and stimulates the release of the gonadotropins LH and FSH into the bloodstream. These gonadotropins regulate the processes in the ovaries, i.e. the multi-stage maturation process of the follicles, ovulation and the development of the corpus luteum, which control the synthesis of the steroids P4 and E2 and of the hormones IhA and IhB. Through the blood, these hormones then reach the hypothalamus and pituitary gland, where they again influence the formation of GnRH, LH and FSH. All model components are listed in Table 1. Except *freq* and *mass*, which are described by algebraic expressions,[1] all components are defined by differential equations.

Since exact mechanisms are often unknown or just too complex, Hill functions are used to model stimulatory (H^+) or inhibitory (H^-) effects:

$$H^+(S(t),T;n)=\frac{(S(t)/T)^n}{1+(S(t)/T)^n},\quad H^-(S(t),T;n)=\frac{1}{1+(S(t)/T)^n}$$

[1] In the Systems Biology Markup Language (SBML), they are defined by assignment rules.

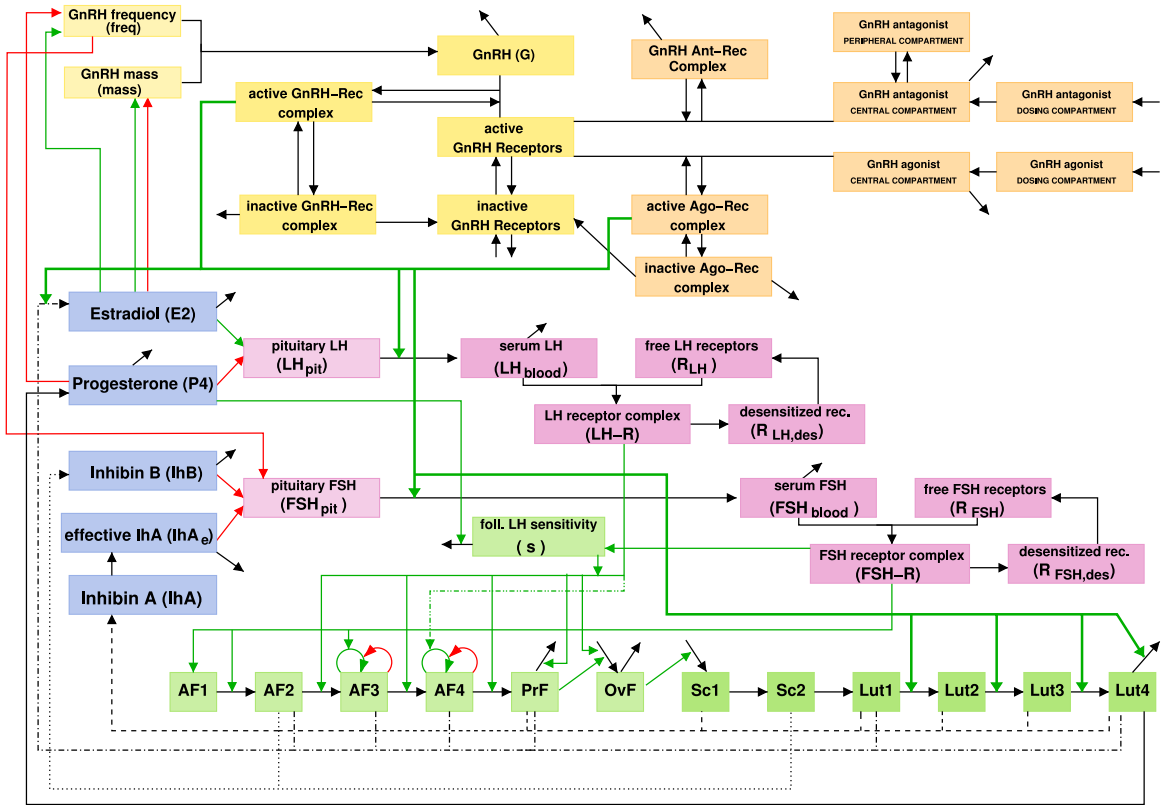

Fig. 1. Flowchart of the model for the female menstrual cycle. Black arrows indicate transitions, elimination, or chemical reactions, green arrows denote stimulatory effects, and red arrows symbolize inhibitory mechanisms. (For interpretation of the references to color in this figure legend, the reader is referred to the web version of this article.)

here $S(t) \geq 0$ denotes the influencing substance, $T > 0$ is the amount of S that causes 50% of the maximum of H^+ or H^-, and $n \geq 1$ is the Hill coefficient, which determines the rate of switching.

The following model equations partially overlap with equations used in the models of Harris (2001), Pasteur (2008) and Reinecke (2009), but have been extended and adapted for the purpose of simulating GnRH analogue treatment. We started with the Reinecke model and performed model reduction and extension. First, we cut off components that coupled only weakly to the rest of the model, such as enzyme reactions in the ovaries. Second, according to Pasteur (2008), the number of follicular phases was extended from 5 to 8 in order to distinguish between IhA and IhB. Moreover, we replaced the stochastic GnRH pulse generator by a deterministic counterpart (more details in Section 2.6).

2.1. Luteinizing hormone (LH)

The gonadotropin equations are based on synthesis–release–clearance relationships. This structure was first introduced by Schlosser and Selgrade (2000). LH-synthesis in the pituitary is stimulated by E2 and inhibited by P4. There is a small constant release rate of LH into the blood (b^{LH}_{Rel}) (Heinze et al., 1998), but the release is mainly stimulated by the GnRH-receptor complex (G-R(t)) and additionally, if present, by the complex between the receptors and the exogenous agonist (Ago-R(t)). This is in line with experimental findings that a low frequency of pulsatile GnRH in women is associated with decreased LH levels and reduced ovulation rate (Filicori et al., 1989). Parameter V_{blood} corresponds to the blood volume. From the blood, unbound LH is reduced by binding to free LH receptors ($k^{\mathrm{LH}}_{on} \cdot \mathrm{R_{LH}}$) or by clearance ($k^{\mathrm{LH}}_{cl}$)

$$Syn_{\mathrm{LH}}(t) = (b^{\mathrm{LH}}_{Syn} + k^{\mathrm{LH}}_{\mathrm{E2}} \cdot H^+(\mathrm{E2}(t), T^{\mathrm{LH}}_{\mathrm{E2}}; n^{\mathrm{LH}}_{\mathrm{E2}})) \cdot H^-(\mathrm{P4}(t), T^{\mathrm{LH}}_{\mathrm{P4}}; n^{\mathrm{LH}}_{\mathrm{P4}}) \quad (1a)$$

$$Rel_{\mathrm{LH}}(t) = (b^{\mathrm{LH}}_{Rel} + k^{\mathrm{LH}}_{\mathrm{G\text{-}R}} \cdot H^+(\mathrm{G\text{-}R}(t) + \mathrm{Ago\text{-}R}(t), T^{\mathrm{LH}}_{\mathrm{G\text{-}R}}; n^{\mathrm{LH}}_{\mathrm{G\text{-}R}})) \cdot \mathrm{LH_{pit}}(t) \quad (1b)$$

$$\frac{d}{dt}\mathrm{LH_{pit}}(t) = Syn_{\mathrm{LH}}(t) - Rel_{\mathrm{LH}}(t) \quad (1)$$

$$\frac{d}{dt}\mathrm{LH}_{blood}(t) = \frac{1}{V_{blood}} \cdot Rel_{\mathrm{LH}}(t) - (k^{\mathrm{LH}}_{on} \cdot \mathrm{R_{LH}}(t) + k^{\mathrm{LH}}_{cl}) \cdot \mathrm{LH}_{blood}(t) \quad (2)$$

2.2. Follicle Stimulating Hormone (FSH)

FSH synthesis is stimulated by low GnRH frequencies (Hall, 2009; Marshall and Griffin, 1993) and inhibited by IhA and IhB (Groome et al., 1996; Hayes et al., 1998; McLachlan et al., 1990; Sehested et al., 2000). Pasteur (2008) modeled these mechanisms by delay differential equations to account for a delayed inhibitory effect of both IhA and IhB. In our model, the timing of FSH synthesis and release is additionally influenced by GnRH. Due to these new mechanisms and the adjustment of rate constants, the delayed effect of IhB could be neglected. The delayed effect of IhA, however, is still important. To avoid the use of delay differential equations, we therefore introduced an effect compartment IhA_e, compare Eq. (28). The release of FSH is proportional to the amount available in the pituitary and additionally stimulated by GnRH, similar to the model in Bertram and Li (2008)

$$Syn_{\mathrm{FSH}}(t) = \frac{k^{\mathrm{FSH}}_{\mathrm{Ih}}}{1 + \left(\frac{\mathrm{IhA}_e}{T_{\mathrm{Ih}A}}\right)^{n_{\mathrm{Ih}A}} + \left(\frac{\mathrm{IhB}}{T_{\mathrm{Ih}B}}\right)^{n_{\mathrm{Ih}B}}} \cdot H^-(\mathrm{freq}, T^{\mathrm{FSH}}_{\mathrm{freq}}; n^{\mathrm{FSH}}_{\mathrm{freq}}) \quad (3a)$$

$$Rel_{\mathrm{FSH}}(t) = (b^{\mathrm{FSH}}_{Rel} + k^{\mathrm{FSH}}_{\mathrm{G\text{-}R}} \cdot H^+(\mathrm{G\text{-}R}(t) + \mathrm{Ago\text{-}R}(t), T^{\mathrm{FSH}}_{\mathrm{G\text{-}R}}; n^{\mathrm{FSH}}_{\mathrm{G\text{-}R}})) \cdot \mathrm{FSH_{pit}}(t) \quad (3b)$$

$$\frac{d}{dt}\mathrm{FSH_{pit}}(t) = Syn_{\mathrm{FSH}}(t) - Rel_{\mathrm{FSH}}(t) \quad (3)$$

Table 1
Model components.

Component	Symbol
LH in the pituitary	LH_{pit}
LH in the blood	LH_{blood}
LH receptors	R_{LH}
LH-receptor-complex	LH-R
Internalized LH receptors	$R_{LH,des}$
FSH in the pituitary	FSH_{pit}
FSH in the blood	FSH_{blood}
FSH receptors	R_{FSH}
FSH-receptor-complex	FSH-R
Internalized FSH receptors	$R_{FSH,des}$
Follicular sensitivity to LH	s
Development stages of antral follicles	AF1/2/3/4
Pre-ovulatory follicular stage	PrF
Ovulatory follicular stage	OvF
Ovulatory scar 1 and 2	Sc1/2
Development stages of corpus luteum	Lut1/2/3/4
Estradiol blood level	E2
Progesterone blood level	P4
Inhibin A blood level	IhA
Inhibin B blood level	IhB
Effective inhibin A	IhA_e
GnRH pulse frequency	freq
GnRH pulse mass	mass
GnRH	G
Active GnRH receptors	$R_{G,a}$
Inactive GnRH receptors	$R_{G,i}$
Active GnRH-receptor complex	$G\text{-}R_a$
Inactive GnRH-receptor complex	$G\text{-}R_i$
GnRH agonist (dosing compartment)	Ago_d
GnRH agonist (central compartment)	Ago_c
Active agonist–receptor complex	$Ago\text{-}R_a$
Inactive agonist–receptor complex	$Ago\text{-}R_i$
GnRH antagonist (dosing comp.)	Ant_d
GnRH antagonist (central comp.)	Ant_c
GnRH antagonist (peripheral comp.)	Ant_p
Antagonist–receptor complex	Ant-R

$$\frac{d}{dt}\mathrm{FSH}_{blood}(t) = \frac{1}{V_{blood}} \cdot Rel_{\mathrm{FSH}}(t) - (k_{on}^{\mathrm{FSH}} \cdot \mathrm{R}_{\mathrm{FSH}}(t) + k_{cl}^{\mathrm{FSH}}) \cdot \mathrm{FSH}_{blood}(t) \tag{4}$$

2.3. LH and FSH receptor binding

Through the blood, LH and FSH reach the ovaries, where they stimulate follicular growth and maturation. The binding of gonadotropins to their receptors activates a cascade of reactions, leading to steroid synthesis.

In Clément et al. (2001), a model for FSH-induced production of cyclic adenosine monophosphate (cAMP) in ovarian follicles has been derived. Here, for simplicity, we only incorporate the therein used receptor recycling into the model. FSH binds to its receptor (R_{FSH}), forming an active complex (FSH-R). Bound receptors are phosphorylated and internalized into the cell, where receptors dissociate from FSH. Internalized receptors ($R_{FSH,des}$) are recycled back to the cell membrane:

$$\mathrm{FSH}_{blood} + \mathrm{R}_{\mathrm{FSH}} \xrightarrow{k_{on}^{\mathrm{FSH}}} \text{FSH-R}_{\mathrm{FSH}}$$

$$\text{FSH-R}_{\mathrm{FSH}} \xrightarrow{k_{des}^{\mathrm{FSH}}} \mathrm{R}_{\mathrm{FSH},des}$$

$$\mathrm{R}_{\mathrm{FSH},des} \xrightarrow{k_{recy}^{\mathrm{FSH}}} \mathrm{R}_{\mathrm{FSH}}$$

Note that, in contrast to Clément et al. (2001), phosphorylation and internalization are summarized in one step (denoted by desensitization) with constant rate k_{des}^{FSH}. The corresponding differential equations read as

$$\frac{d}{dt}\mathrm{R}_{\mathrm{FSH}}(t) = k_{recy}^{\mathrm{FSH}} \cdot \mathrm{R}_{\mathrm{FSH},des}(t) - k_{on}^{\mathrm{FSH}} \cdot \mathrm{FSH}_{blood}(t) \cdot \mathrm{R}_{\mathrm{FSH}}(t) \tag{5}$$

$$\frac{d}{dt}\text{FSH-R}(t) = k_{on}^{\mathrm{FSH}} \cdot \mathrm{FSH}_{blood}(t) \cdot \mathrm{R}_{\mathrm{FSH}}(t) - k_{des}^{\mathrm{FSH}} \cdot \text{FSH-R}(t) \tag{6}$$

$$\frac{d}{dt}\mathrm{R}_{\mathrm{FSH},des}(t) = k_{des}^{\mathrm{FSH}} \cdot \text{FSH-R}(t) - k_{recy}^{\mathrm{FSH}} \cdot \mathrm{R}_{\mathrm{FSH},des}(t) \tag{7}$$

We deliberately did not introduce reversible receptor binding, which would have just increased the number of unknown parameters without overall benefit. As in Clément et al. (2001), we assume that the total number of FSH receptors remains constant

$$\mathrm{R}_{\mathrm{FSH}}(t) + \text{FSH-R}(t) + \mathrm{R}_{\mathrm{FSH},des}(t) = \text{constant}$$

This number is determined by the sum of the corresponding initial values. This allows for replacing one of the receptor states by the difference between total receptor number and the sum of the other states, thus reducing the number of differential equations.

Since both FSH and LH operate mainly through the same receptor binding mechanisms, we model the LH receptor dynamics similar to FSH:

$$\mathrm{LH}_{blood} + \mathrm{R}_{\mathrm{LH}} \xrightarrow{k_{on}^{\mathrm{LH}}} \text{LH-R}$$

$$\text{LH-R} \xrightarrow{k_{des}^{\mathrm{LH}}} \mathrm{R}_{\mathrm{LH},des}$$

$$\mathrm{R}_{\mathrm{LH},des} \xrightarrow{k_{recy}^{\mathrm{LH}}} \mathrm{R}_{\mathrm{LH}}$$

The corresponding differential equations read as

$$\frac{d}{dt}\mathrm{R}_{\mathrm{LH}}(t) = k_{recy}^{\mathrm{LH}} \cdot \mathrm{R}_{\mathrm{LH},des}(t) - k_{on}^{\mathrm{LH}} \cdot \mathrm{LH}_{blood}(t) \cdot \mathrm{R}_{\mathrm{LH}}(t) \tag{8}$$

$$\frac{d}{dt}\text{LH-R}(t) = k_{on}^{\mathrm{LH}} \cdot \mathrm{LH}_{blood}(t) \cdot \mathrm{R}_{\mathrm{LH}}(t) - k_{des}^{\mathrm{LH}} \cdot \text{LH-R}(t) \tag{9}$$

$$\frac{d}{dt}\mathrm{R}_{\mathrm{LH},des}(t) = k_{des}^{\mathrm{LH}} \cdot \text{LH-R}(t) - k_{recy}^{\mathrm{LH}} \cdot \mathrm{R}_{\mathrm{LH},des}(t) \tag{10}$$

Again, the total receptor number is constant, which reduces the number of equations by one.

2.4. Development of follicles and corpus luteum

The model for the development of follicles is adapted from Pasteur (2008), but we slightly changed the notation of the different developmental stages. The model includes the development from antral follicles (AF) to preovulatory follicles (PrF), i.e. the follicular phase of the menstrual cycle in which (usually five to seven) selected antral follicles compete with each other for growth-inducing FSH (Macklon and Fauser, 2001; Zeleznik, 2004). In our model, the antral follicles are divided into four different stages of development, AF1 to AF4. These variables should not be interpreted as size or number of follicles, but as stage of maturation and thus as ability to produce steroid hormones. During the mid through late follicular phase, FSH induces the increase of LH receptors in follicular granulosa cells, which makes the follicles less dependent on declining FSH concentrations (Zeleznik, 2004; Zeleznik and Pohl, 2006). To account for this effect, we introduce a new variable, $s(t)$, as the sensitivity of follicles to LH, i.e. the level of response to certain amounts of LH. $s(t)$ is stimulated by FSH, and decreases with the sustained development of the corpus luteum, represented by increasing amounts of P4:

$$\frac{d}{dt}s(t) = k^s \cdot H^+(\mathrm{FSH}(t), T_{\mathrm{FSH}}^s; n_{\mathrm{FSH}}^s) - k_{cl}^s \cdot H^+(\mathrm{P4}(t), T_{\mathrm{P4}}^s; n_{\mathrm{P4}}^s) \cdot s(t) \tag{11}$$

All LH dependent transition rates between different follicular stages are multiplied with $s(t)$. Thus, the influence of LH is diminished when $s(t)$ is small. This results in different effects of an LH peak (caused by GnRH agonist treatment) in the early and late follicular phase.

The corpus luteum starts to develop under the condition that there is an LH peak and the follicles are ready for ovulation (Niswender et al., 2000). Therefore, an ovulatory follicle only develops when the preovulatory follicle is mature enough; an LH peak in the early follicular phase does not cause ovulation (Monroe et al., 1985). To make the ovulatory scar independent of the size of the ovulatory follicle, its growth only depends on OvF via a Hill function. Thus, a normal luteal function is maintained even if ovulation has been enforced earlier, e.g. by GnRH agonist treatment in the late follicular phase.

According to Tavaniotou et al. (2001), a direct effect of the GnRH agonist or GnRH antagonist on human corpus luteum or on human endometrium and thus on endometrial receptivity cannot be excluded, as GnRH receptors have been described in both compartments (Bramley and Menzies, 1986). In the corpus luteum, GnRH-I, GnRH-II, and GnRH receptors were observed in granulosa luteal cells but not in theca luteal cells (Metallinou et al., 2007). GnRH-I has been suggested as a luteolytic factor, increasing the number of apoptotic luteinized granulosa cells (Zhao et al., 2000). We thus decided to model the luteolytic effect of GnRH agonist treatment by including a stimulatory effect of the active GnRH-receptor complex on the transitions between different luteal stages. This modification accounts for a truncated luteal phase after agonist administration in the late luteal phase.

Summarizing, we arrive at the following set of differential equations:

$$\frac{d}{dt}\mathrm{AF1}(t) = k^{\mathrm{AF1}}\cdot H^{+}(\mathrm{FSH\text{-}R}(t), T^{\mathrm{AF1}}_{\mathrm{FSH\text{-}R}}; n^{\mathrm{AF1}}_{\mathrm{FSH\text{-}R}}) - k^{\mathrm{AF2}}_{\mathrm{AF1}}\cdot \mathrm{FSH\text{-}R}(t)\cdot \mathrm{AF1}(t) \tag{12}$$

$$\begin{aligned}\frac{d}{dt}\mathrm{AF2}(t) = {} & k^{\mathrm{AF2}}_{\mathrm{AF1}}\cdot \mathrm{FSH\text{-}R}(t)\cdot \mathrm{AF1}(t)\\ & - k^{\mathrm{AF3}}_{\mathrm{AF2}}\cdot (\mathrm{LH\text{-}R}(t)/SF_{\mathrm{LH}}R)^{n^{\mathrm{AF3}}_{\mathrm{AF2}}}\cdot s(t)\cdot \mathrm{AF2}(t)\end{aligned} \tag{13}$$

$$\begin{aligned}\frac{d}{dt}\mathrm{AF3}(t) = {} & k^{\mathrm{AF3}}_{\mathrm{AF2}}\cdot (\mathrm{LH\text{-}R}(t)/SF_{\mathrm{LH}}R)^{n^{\mathrm{AF3}}_{\mathrm{AF2}}}\cdot s(t)\cdot \mathrm{AF2}(t)\\ & + k^{\mathrm{AF3}}_{\mathrm{AF3}}\cdot \mathrm{FSH\text{-}R}(t)\cdot \mathrm{AF3}(t)\cdot (1-\mathrm{AF3}(t)/SeF_{\max})\\ & - k^{\mathrm{AF4}}_{\mathrm{AF3}}\cdot (\mathrm{LH\text{-}R}(t)/SF_{\mathrm{LH}}R)^{n^{\mathrm{AF4}}_{\mathrm{AF3}}}\cdot s(t)\cdot \mathrm{AF3}(t)\end{aligned} \tag{14}$$

$$\begin{aligned}\frac{d}{dt}\mathrm{AF4}(t) = {} & k^{\mathrm{AF4}}_{\mathrm{AF3}}\cdot (\mathrm{LH\text{-}R}(t)/SF_{\mathrm{LH}}R)^{n^{\mathrm{AF4}}_{\mathrm{AF3}}}\cdot s(t)\cdot \mathrm{AF3}(t)\\ & + k^{\mathrm{AF4}}_{\mathrm{AF4}}\cdot (\mathrm{LH\text{-}R}(t)/SF_{\mathrm{LH}}R)^{n^{\mathrm{AF4}}}\cdot \mathrm{AF4}(t)\cdot (1-\mathrm{AF4}(t)/SeF_{\max})\\ & - k^{\mathrm{PrF}}_{\mathrm{AF4}}\cdot (\mathrm{LH\text{-}R}(t)/SF_{\mathrm{LH}}R)\cdot s(t)\cdot \mathrm{AF4}(t)\end{aligned} \tag{15}$$

$$\begin{aligned}\frac{d}{dt}\mathrm{PrF}(t) = {} & k^{\mathrm{PrF}}_{\mathrm{AF4}}\cdot (\mathrm{LH\text{-}R}(t)/SF_{\mathrm{LH}}R)\cdot s(t)\cdot \mathrm{AF4}(t)\\ & - k^{\mathrm{PrF}}_{cl}\cdot (\mathrm{LH\text{-}R}(t)/SF_{\mathrm{LH}}R)^{n^{\mathrm{OvF}}}\cdot s(t)\cdot \mathrm{PrF}(t)\end{aligned} \tag{16}$$

$$\begin{aligned}\frac{d}{dt}\mathrm{OvF}(t) = {} & k^{\mathrm{OvF}}\cdot (\mathrm{LH\text{-}R}(t)/SF_{\mathrm{LH}}R)^{n^{\mathrm{OvF}}}\cdot s(t)\cdot H^{+}(\mathrm{PrF}(t), T^{\mathrm{OvF}}_{\mathrm{PrF}}; n^{\mathrm{OvF}}_{\mathrm{PrF}})\\ & - k^{\mathrm{OvF}}_{cl}\cdot \mathrm{OvF}(t)\end{aligned} \tag{17}$$

$$\frac{d}{dt}\mathrm{Sc1}(t) = k^{\mathrm{Sc1}}\cdot H^{+}(\mathrm{OvF}(t), T^{\mathrm{Sc1}}_{\mathrm{OvF}}, n^{\mathrm{Sc1}}_{\mathrm{OvF}}) - k^{\mathrm{Sc2}}_{\mathrm{Sc1}}\cdot \mathrm{Sc1}(t) \tag{18}$$

$$\frac{d}{dt}\mathrm{Sc2}(t) = k^{\mathrm{Sc2}}_{\mathrm{Sc1}}\cdot \mathrm{Sc1}(t) - k^{\mathrm{Lut1}}_{\mathrm{Sc2}}\cdot \mathrm{Sc2}(t) \tag{19}$$

$$\begin{aligned}\frac{d}{dt}\mathrm{Lut1}(t) = {} & k^{\mathrm{Lut1}}_{\mathrm{Sc2}}\cdot \mathrm{Sc2}(t)\\ & - k^{\mathrm{Lut2}}_{\mathrm{Lut1}}\cdot (1+m^{\mathrm{Lut}}_{\mathrm{G\text{-}R}}\cdot H^{+}(\mathrm{G\text{-}R}_a(t), T^{\mathrm{Lut}}_{\mathrm{G\text{-}R}}; n^{\mathrm{Lut}}_{\mathrm{G\text{-}R}}))\cdot \mathrm{Lut1}(t)\end{aligned} \tag{20}$$

$$\begin{aligned}\frac{d}{dt}\mathrm{Lut2}(t) = {} & k^{\mathrm{Lut2}}_{\mathrm{Lut1}}\cdot (1+m^{\mathrm{Lut}}_{\mathrm{G\text{-}R}}\cdot H^{+}(\mathrm{G\text{-}R}_a(t), T^{\mathrm{Lut}}_{\mathrm{G\text{-}R}}; n^{\mathrm{Lut}}_{\mathrm{G\text{-}R}}))\cdot \mathrm{Lut1}(t)\\ & - k^{\mathrm{Lut3}}_{\mathrm{Lut2}}\cdot (1+m^{\mathrm{Lut}}_{\mathrm{G\text{-}R}}\cdot H^{+}(\mathrm{G\text{-}R}_a(t), T^{\mathrm{Lut}}_{\mathrm{G\text{-}R}}; n^{\mathrm{Lut}}_{\mathrm{G\text{-}R}}))\cdot \mathrm{Lut2}(t)\end{aligned} \tag{21}$$

$$\begin{aligned}\frac{d}{dt}\mathrm{Lut3}(t) = {} & k^{\mathrm{Lut3}}_{\mathrm{Lut2}}(1+m^{\mathrm{Lut}}_{\mathrm{G\text{-}R}}\cdot H^{+}(\mathrm{G\text{-}R}_a(t), T^{\mathrm{Lut}}_{\mathrm{G\text{-}R}}; n^{\mathrm{Lut}}_{\mathrm{G\text{-}R}}))\cdot \mathrm{Lut2}(t)\\ & - k^{\mathrm{Lut4}}_{\mathrm{Lut3}}\cdot (1+m^{\mathrm{Lut}}_{\mathrm{G\text{-}R}}\cdot H^{+}(\mathrm{G\text{-}R}_a(t), T^{\mathrm{Lut}}_{\mathrm{G\text{-}R}}; n^{\mathrm{Lut}}_{\mathrm{G\text{-}R}}))\cdot \mathrm{Lut3}(t)\end{aligned} \tag{22}$$

$$\begin{aligned}\frac{d}{dt}\mathrm{Lut4}(t) = {} & k^{\mathrm{Lut4}}_{\mathrm{Lut3}}(1+m^{\mathrm{Lut}}_{\mathrm{G\text{-}R}}\cdot H^{+}(\mathrm{G\text{-}R}_a(t), T^{\mathrm{Lut}}_{\mathrm{G\text{-}R}}; n^{\mathrm{Lut}}_{\mathrm{G\text{-}R}}))\cdot \mathrm{Lut3}(t)\\ & - k^{\mathrm{Lut4}}_{cl}\cdot (1+m^{\mathrm{Lut}}_{\mathrm{G\text{-}R}}\cdot H^{+}(\mathrm{G\text{-}R}_a(t), T^{\mathrm{Lut}}_{\mathrm{G\text{-}R}}; n^{\mathrm{Lut}}_{\mathrm{G\text{-}R}}))\cdot \mathrm{Lut4}(t)\end{aligned} \tag{23}$$

2.5. Estradiol (E2), progesterone (P4) and inhibins (IhA,IhB)

E2, P4, IhA and IhB are produced by the follicles and/or the corpus luteum (Magoffin and Jakimiuk, 1997; Niswender et al., 2000; Macklon and Fauser, 2001; Strauss, 2009). Published data sets in Welt et al. (1999) indicate that IhA has a peak shortly before ovulation and is mainly produced in the luteal phase, whereas IhB is high in the mid follicular phase, with an additional peak around ovulation. The production of estradiol is stimulated by LH since LH induces androgen synthesis, which is converted into estradiol by aromatase enzymes (Strauss, 1999). The ovarian hormone concentrations are related to the ovarian development stages by linear equations:

$$\begin{aligned}\frac{d}{dt}\mathrm{E2}(t) = {} & b^{\mathrm{E2}} + k^{\mathrm{E2}}_{\mathrm{AF2}}\cdot \mathrm{AF2}(t) + k^{\mathrm{E2}}_{\mathrm{AF3}}\cdot \mathrm{LH}(t)\cdot \mathrm{AF3}(t) + k^{\mathrm{E2}}_{\mathrm{AF4}}\cdot \mathrm{AF4}(t)\\ & + k^{\mathrm{E2}}_{\mathrm{PrF}}\cdot \mathrm{LH}(t)\cdot \mathrm{PrF} + k^{\mathrm{E2}}_{\mathrm{Lut1}}\cdot \mathrm{Lut1}(t)\\ & + k^{\mathrm{E2}}_{\mathrm{Lut4}}\cdot \mathrm{Lut4}(t) - k^{\mathrm{E2}}_{cl}\cdot \mathrm{E2}(t)\end{aligned} \tag{24}$$

$$\frac{d}{dt}\mathrm{P4}(t) = b^{\mathrm{P4}} + k^{\mathrm{P4}}_{\mathrm{Lut4}}\cdot \mathrm{Lut4}(t) - k^{\mathrm{P4}}_{cl}\cdot \mathrm{P4}(t) \tag{25}$$

$$\begin{aligned}\frac{d}{dt}\mathrm{IhA}(t) = {} & b^{\mathrm{IhA}} + k^{\mathrm{IhA}}_{\mathrm{PrF}}\cdot \mathrm{PrF}(t) + k^{\mathrm{IhA}}_{\mathrm{Sc1}}\cdot \mathrm{Sc1}(t) + k^{\mathrm{IhA}}_{\mathrm{Lut1}}\cdot \mathrm{Lut1}(t) + k^{\mathrm{IhA}}_{\mathrm{Lut2}}\cdot \mathrm{Lut2}(t)\\ & + k^{\mathrm{IhA}}_{\mathrm{Lut3}}\cdot \mathrm{Lut3}(t) + k^{\mathrm{IhA}}_{\mathrm{Lut4}}\cdot \mathrm{Lut4}(t) - k^{\mathrm{IhA}}\cdot \mathrm{IhA}(t)\end{aligned} \tag{26}$$

$$\frac{d}{dt}\mathrm{IhB}(t) = b^{\mathrm{IhB}} + k^{\mathrm{IhB}}_{\mathrm{AF2}}\cdot \mathrm{AF2}(t) + k^{\mathrm{IhB}}_{\mathrm{Sc2}}\cdot \mathrm{Sc2}(t) - k^{\mathrm{IhB}}_{cl}\cdot \mathrm{IhB}(t) \tag{27}$$

To account for a delayed effect of IhA on FSH synthesis and to avoid the use of delay differential equations, we additionally introduce an effect compartment:

$$\frac{d}{dt}\mathrm{IhA}_e(t) = k^{\mathrm{IhA}}\cdot \mathrm{IhA}(t) - k^{\mathrm{IhA}_e}_{cl}\cdot \mathrm{IhA}_e(t) \tag{28}$$

As illustrated by the simulation results in Section 3, effective inhibin A attains its maximum about 3 days after the maximum of IhA. Thus, the time-delay in the effect of IhA as reported in literature (Ramaswamy et al., 1998; Margolskee and Selgrade, 2011) is present in the model.

2.6. Gonadotropin releasing hormone GnRH (G)

Even though elaborate mathematical models for the GnRH pulse generator are available (Brown et al., 1994; Keenan et al., 2000; Vidal and Clément, 2010), we deliberately abandoned these mechanisms from our model because they act on a smaller time scale (minutes) than the one we are interested in (days). On the

one hand, the model would become more accurate by adding this level of detail. On the other hand, it would significantly increase the simulation time by many orders of magnitude due to the requirement of small computational timesteps in the numerical integrator. Therefore, we decided to include only GnRH pulse frequency (freq) and amount of released GnRH (mass) in our model. If wanted, the pulse pattern of GnRH can be computed from the frequency, but this is not within the scope of our present model.

GnRH frequency is inhibited by P4 and stimulated by E2 (Chabbert-Buffet and Bouchard, 2002; Swerdloff et al., 1972; Hall, 2009). It is well known that E2 suppresses GnRH pulse size and secretion from the hypothalamus despite its stimulatory action on GnRH pulse frequency (Evans et al., 1994). However, in the late follicular phase, the feedback action of estradiol switches to positive, thus inducing the GnRH surge (Christen and Moenter, 2010). We decided to include a stimulatory effect of high E2 concentrations on GnRH pulse mass to account for this effect without going into the details of neurosecretion, which would have gone beyond the scope of this paper. In fact, the influence of E2 on GnRH neurons is manifold and species-specific (Herbison, 1998), and the mechanisms are not yet fully established

$$\mathrm{freq}(t) = f_0 \cdot H^-(\mathrm{P4}(t), T_{\mathrm{P4}}^{\mathrm{freq}}; n_{\mathrm{P4}}^{\mathrm{freq}}) \cdot (1 + m_{\mathrm{E2}}^{\mathrm{freq}} \cdot H^+(\mathrm{E2}(t), T_{\mathrm{E2}}^{\mathrm{freq}}; n_{\mathrm{E2}}^{\mathrm{freq}})) \tag{29a}$$

$$\mathrm{mass}(t) = a_0 \cdot (H^+(\mathrm{E2}(t), T_{\mathrm{E2}}^{\mathrm{mass},1}; n_{\mathrm{E2}}^{\mathrm{mass},1}) + H^-(\mathrm{E2}(t), T_{\mathrm{E2}}^{\mathrm{mass},2}; n_{\mathrm{E2}}^{\mathrm{mass},2})) \tag{29b}$$

$$\frac{d}{dt}\mathrm{G}(t) = \mathrm{mass}(t) \cdot \mathrm{freq}(t) - k_{on}^{G} \cdot \mathrm{G}(t) \cdot \mathrm{R}_{\mathrm{G,a}}(t) + k_{off}^{G} \cdot \mathrm{G\text{-}R}_a(t) - k_{degr}^{G} \cdot \mathrm{G}(t) \tag{29}$$

The GnRH receptor belongs to the class of G-protein coupled receptors (GPCR). We therefore adapted a GPCR model from Riccobene et al. (1999) and Shankaran et al. (2007). Our model for GnRH receptor binding is illustrated in Fig. 2. In the pituitary, there is a number of active GnRH receptors ($\mathrm{R_{G,a}}$) on the cell surface, available for binding, as well as a pool of inactive GnRH receptors ($\mathrm{R_{G,i}}$) inside the cell. The receptors are reversibly internalized and recycled with rates $k_{inter}^{\mathrm{R_G}}$ and $k_{recy}^{\mathrm{R_G}}$. The model includes binding of active receptors to GnRH with forward rate k_{on}^{G} and reverse-rate k_{off}^{G}. The active GnRH-receptor complex ($\mathrm{G\text{-}R}_a$) is reversibly inactivated (internalized) with rate $k_{inact}^{\mathrm{G\text{-}R}}$ and reactivated with rate $k_{act}^{\mathrm{G\text{-}R}}$ to yield an inactive complex ($\mathrm{G\text{-}R}_i$). The inactive complex is degraded with rate $k_{degr}^{\mathrm{G\text{-}R}_i}$ or it irreversibly dissociates inside the cell with rate $k_{diss}^{\mathrm{G\text{-}R}_i}$, bringing new inactive GnRH receptors ($\mathrm{R_{G,i}}$) into the pool (desensitization). To avoid a loss of receptors due to desensitization, the model also includes a permanent synthesis and degradation of inactive receptors.

The differential equations corresponding to the above-described reaction scheme are described as follows:

$$\frac{d}{dt}\mathrm{R_{G,a}}(t) = k_{off}^{G} \cdot \mathrm{G\text{-}R}_a(t) - k_{on}^{G} \cdot \mathrm{G}(t) \cdot \mathrm{R_{G,a}}(t) - k_{inter}^{\mathrm{R_G}} \cdot \mathrm{R_{G,a}}(t) + k_{recy}^{\mathrm{R_G}} \mathrm{R_{G,i}} \tag{30}$$

$$\frac{d}{dt}\mathrm{R_{G,i}}(t) = k_{diss}^{\mathrm{G\text{-}R}_i} \cdot \mathrm{G\text{-}R}_i(t) + k_{inter}^{\mathrm{R_G}} \cdot \mathrm{R_{G,a}}(t) - k_{recy}^{\mathrm{R_G}} \mathrm{R_{G,i}}(t) + k_{syn}^{\mathrm{R_{G,i}}} - k_{degr}^{\mathrm{R_{G,i}}} \cdot \mathrm{R_{G,i}}(t) \tag{31}$$

$$\frac{d}{dt}\mathrm{G\text{-}R}_a(t) = k_{on}^{G} \cdot \mathrm{G}(t) \cdot \mathrm{R_{G,a}}(t) - k_{off}^{G} \cdot \mathrm{G\text{-}R}_a(t) - k_{inact}^{\mathrm{G\text{-}R}} \cdot \mathrm{G\text{-}R}_a(t) + k_{act}^{\mathrm{G\text{-}R}} \mathrm{G\text{-}R}_i(t) \tag{32}$$

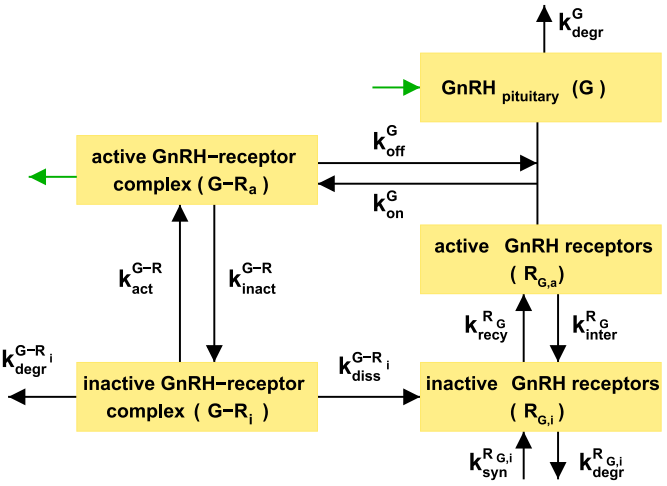

Fig. 2. GnRH receptor binding model as zoom from the large model, see upper left part of Fig. 1.

$$\frac{d}{dt}\mathrm{G\text{-}R}_i(t) = k_{inact}^{\mathrm{G\text{-}R}} \cdot \mathrm{G\text{-}R}_a(t) - k_{act}^{\mathrm{G\text{-}R}} \mathrm{G\text{-}R}_i(t) - k_{degr}^{\mathrm{G\text{-}R}_i} \cdot \mathrm{G\text{-}R}_i(t) - k_{diss}^{\mathrm{G\text{-}R}_i} \cdot \mathrm{G\text{-}R}_i(t) \tag{33}$$

Even though this model is simple, it can capture the essential features of the GnRH system. For example, the model takes into account the fluctuation of the receptor between active and inactive conformations, a fundamental process in GnRH signaling. Furthermore, it has been well established that the mammalian GnRH receptor is a very particular GPCR, in that it lacks the intracytoplasmic C-terminal tail, a structure implicated in desensitization and internalization of many GPCRs (McArdle et al., 2002). As a consequence, GnRH receptors do not undergo rapid homologous receptor desensitization nor do they rapidly internalize (Bliss et al., 2010; Naor, 2009). The model presented here can account for these facts by choosing small values for $k_{act}^{\mathrm{G\text{-}R}}$ and/or $k_{diss}^{\mathrm{G\text{-}R}_i}$. Moreover, the values of the rate constants may change depending on the ligand, according to the concept of ligand-induced selective signaling (Millar et al., 2004).

2.7. Administration of GnRH agonist Nafarelin

Fig. 3 shows a diagrammatic representation of the compartmental model developed to describe the PK/PD model of the GnRH agonist Nafarelin. Since the data for plasma drug concentration exhibit an exponential decay, we decided to model the administration of Nafarelin via a classical one-compartmental first-order absorption model (Bourne, 1995). The drug is administered directly into the dosing compartment from where it is transported into the central compartment and cleared:

$$\mathrm{Ago_d} \xrightarrow{k_A^{\mathrm{Ago}}} \mathrm{Ago_c} \xrightarrow{cl^{\mathrm{Ago}}} *$$

$\mathrm{Ago_d}$ is the amount of agonist in the dosing compartment and $\mathrm{Ago_c}$ the concentration in the central compartment. Here and in the following, the $*$ represents a component without feedback to the rest of the system, which can therefore be neglected during the simulation.

The agonist concentration in the dosing compartment is determined by first-order absorption:

$$\frac{d}{dt}\mathrm{Ago_d}(t) = -k_A^{\mathrm{Ago}} \cdot \mathrm{Ago_d}(t) \tag{34}$$

At the time points of dosing, $\{t_{D,i}\}_{i=1}^{n}$, the dose D_{Ago} is added to $\mathrm{Ago_d}(t)$.

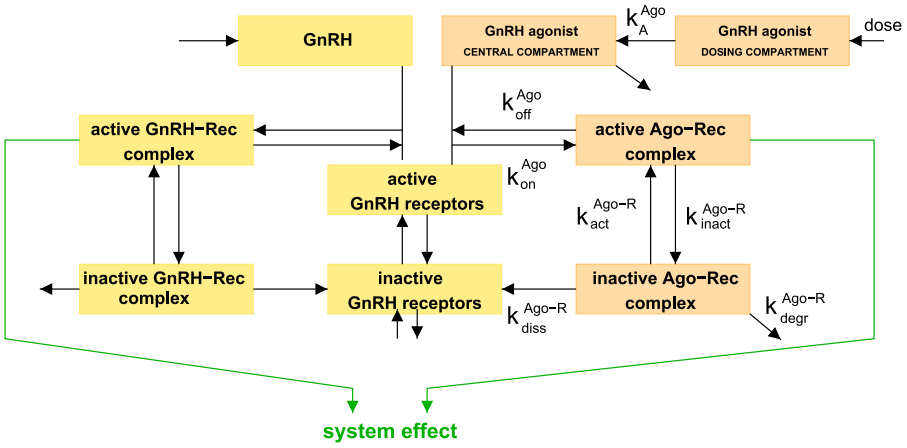

Fig. 3. Diagrammatic representation of the compartmental model developed to describe the PK/PD model of the GnRH agonist Nafarelin.

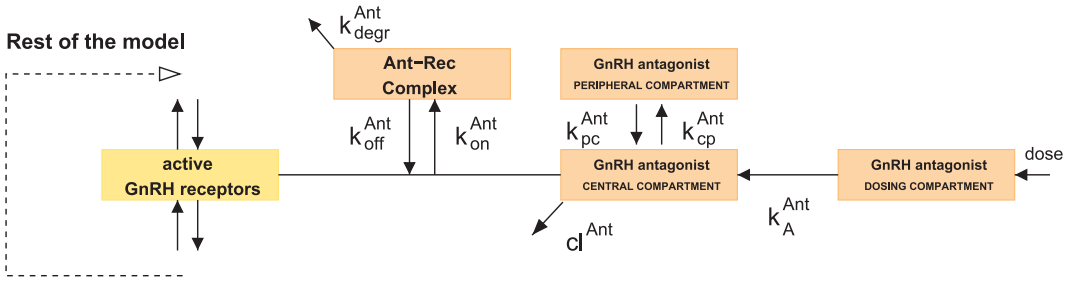

Fig. 4. Diagrammatic representation of the compartmental model developed to describe the PK/PD model of the GnRH antagonist Cetrorelix.

Since only the free drug in the central compartment is available for binding to the GnRH receptor, we multiply the amount of agonist that reaches the central compartment from the dosing compartment with the bioavailability F^{Ago}. Moreover, the agonist amount is diluted with respect to the volume of the central compartment (V_c). The preliminary differential equation for the agonist concentration in the central compartment is

$$\frac{d}{dt}\mathrm{Ago_c}(t) = k_A^{\mathrm{Ago}} \cdot \mathrm{Ago_d}(t) \cdot F^{\mathrm{Ago}}/V_c - cl^{\mathrm{Ago}} \cdot \mathrm{Ago_c}(t) \tag{35}$$

The coupling of the PK equations to the rest of the model occurs via reaction-rate equations. The agonist binds via a reversible reaction to active GnRH receptors on the cell surface and forms an active complex (Ago-R_a), which is acting in the same way as the active GnRH-receptor complex. That means, the complex gets internalized and recycled in a reversible way. The inactive complex (Ago-R_i) is degraded or dissociated into a pool of inactive GnRH receptors inside the cell. The reaction scheme is

$$\mathrm{Ago_c} + \mathrm{R_{G,a}} \underset{k_{off}^{\mathrm{Ago}}}{\overset{k_{on}^{\mathrm{Ago}}}{\rightleftharpoons}} \text{Ago-R}_a, \qquad \text{Ago-R}_a \underset{k_{inact}^{\text{Ago-R}}}{\overset{k_{act}^{\text{Ago-R}}}{\rightleftharpoons}} \text{Ago-R}_i$$

$$\text{Ago-R}_i \overset{k_{degr}^{\text{Ago-R}}}{\longrightarrow} *, \qquad \text{Ago-R}_i \overset{k_{diss}^{\text{Ago-R}}}{\longrightarrow} \mathrm{R_{G,i}}$$

The concentrations of active and inactive agonist–receptor complex are calculated as:

$$\frac{d}{dt}\text{Ago-R}_a(t) = k_{on}^{\mathrm{Ago}} \cdot SF_{\mathrm{Ago}} \cdot \mathrm{R_{G,a}}(t) \cdot \mathrm{Ago_c}(t) - k_{off}^{\mathrm{Ago}} \cdot \text{Ago-R}_a(t) + k_{act}^{\mathrm{Ago}} R \cdot \text{Ago-R}_i(t) - k_{inact}^{\mathrm{Ago}} R \cdot \mathrm{R_{G,a}}(t) \cdot \text{Ago-R}_a(t) \tag{36}$$

$$\frac{d}{dt}\text{Ago-R}_i(t) = k_{inact}^{\mathrm{Ago}} R \cdot \mathrm{R_{G,a}}(t) \cdot \text{Ago-R}_a(t) - k_{act}^{\mathrm{Ago}} R \cdot \text{Ago-R}_i(t) - k_{diss}^{\mathrm{Ago}} R \cdot \text{Ago-R}_i(t) - k_{degr}^{\mathrm{Ago}} R \cdot \text{Ago-R}_i(t) \tag{37}$$

The scaling factor SF_{Ago} accounts for the conversion of units from the agonist in the central compartment (ng/mL) to the concentration of agonist–receptor complex (nmol/mL). The effect of the agonist–receptor complex is added to the effect of the GnRH-receptor complex wherever it appears (cf. Rel_{LH}, Rel_{FSH}, CL development, E2).

Since the binding is reversible, it also affects the equation for the agonist in the central compartment:

$$\frac{d}{dt}\mathrm{Ago_c}(t) = k_A^{\mathrm{Ago}} \cdot \mathrm{Ago_d}(t) \cdot F^{\mathrm{Ago}}/V_c - cl^{\mathrm{Ago}} \cdot \mathrm{Ago_c}(t) - k_{on}^{\mathrm{Ago}} \cdot \mathrm{R_{G,a}}(t) \cdot \mathrm{Ago_c}(t) + k_{off}^{\mathrm{Ago}}/SF_{\mathrm{Ago}} \cdot \text{Ago-R}_a(t) \tag{35*}$$

Finally, the equations for both the active and the inactive GnRH receptors have to be modified:

$$\frac{d}{dt}\mathrm{R_{G,a}}(t) = k_{off}^{G} \cdot \text{G-R}(t) - k_{on}^{G} \cdot \mathrm{G}(t) \cdot \mathrm{R_{G,a}}(t) - k_{inter}^{\mathrm{R_G}} \cdot \mathrm{R_{G,a}}(t) + k_{recy}^{\mathrm{R_G}} \mathrm{R_{G,i}} - k_{on}^{\mathrm{Ago}} \cdot SF_{\mathrm{Ago}} \cdot \mathrm{Ago_c}(t) \cdot \mathrm{R_{G,a}}(t) + k_{off}^{\mathrm{Ago}} \cdot \text{Ago-R}(t), \tag{30*}$$

$$\frac{d}{dt}\mathrm{R_{G,i}}(t) = k_{diss}^{\text{G-R}_i} \cdot \text{G-R}_i(t) + k_{inter}^{\mathrm{R_G}} \cdot \mathrm{R_{G,a}}(t) - k_{recy}^{\mathrm{R_G}} \mathrm{R_{G,i}}(t) + k_{syn}^{\mathrm{R_G}} - k_{degr}^{\mathrm{R_G}} \cdot \mathrm{R_{G,i}}(t) + k_{diss}^{\mathrm{Ago}} \cdot \text{Ago-R}_a(t) \tag{31*}$$

2.8. Administration of GnRH antagonist Cetrorelix

Fig. 4 shows a diagrammatic representation of the compartmental model developed to describe the PK/PD model of the GnRH antagonist Cetrorelix. Administration of Cetrorelix is modeled via a classical two-compartmental first-order absorption model (Bourne, 1995). We chose this approach to account for a bi-exponential decrease in plasma drug concentration over time. The drug is administered directly into the dosing compartment

from where it is transported into the central compartment. A certain amount of drug reaches the peripheral compartment, from where it is gradually absorbed back into the central compartment (Fig. 4):

$$\mathrm{Ant_d} \xrightarrow{k_A^{\mathrm{Ant}}} \mathrm{Ant_c} \underset{k_{pc}^{\mathrm{Ant}}}{\overset{k_{cp}^{\mathrm{Ant}}}{\rightleftharpoons}} \mathrm{Ant_p}, \quad \mathrm{Ant_c} \xrightarrow{cl^{\mathrm{Ant}}} *$$

$\mathrm{Ant_d}$ is the amount of antagonist in the dosing compartment, $\mathrm{Ant_c}$ the concentration in the central, and $\mathrm{Ant_p}$ the concentration in the peripheral compartment. The equations for the antagonist PK model are similar to the agonist PK model, only the peripheral compartment is added:

$$\frac{d}{dt}\mathrm{Ant_d}(t) = -k_A^{\mathrm{Ant}} \cdot \mathrm{Ant_d}(t) \tag{38}$$

$$\frac{d}{dt}\mathrm{Ant_c}(t) = k_A^{\mathrm{Ant}} \cdot \mathrm{Ant_d}(t) \cdot F^{\mathrm{Ant}}/V_c - cl^{\mathrm{Ant}} \cdot \mathrm{Ant_c}(t) - k_{cp}^{\mathrm{Ant}} \cdot \mathrm{Ant_c}(t) + k_{pc}^{\mathrm{Ant}} \cdot \mathrm{Ant_p}(t) \tag{39}$$

$$\frac{d}{dt}\mathrm{Ant_p}(t) = k_{cp}^{\mathrm{Ant}} \cdot \mathrm{Ant_c}(t) - k_{pc}^{\mathrm{Ant}} \cdot \mathrm{Ant_p}(t) \tag{40}$$

At the time points of dosing, $\{t_{D,i}\}_{i=1}^{n}$, the dose D_{Ant} is added to $\mathrm{Ant_d}(t)$.

In contrast to the agonist, the GnRH receptor is not activated by binding to the antagonist. Therefore, we consider only the following reactions:

$$\mathrm{Ant_c} + \mathrm{R_{G,a}} \underset{k_{off}^{\mathrm{Ant}}}{\overset{k_{on}^{\mathrm{Ant}}}{\rightleftharpoons}} \text{Ant-R}, \quad \text{Ant-R} \xrightarrow{k_{degr}^{\mathrm{Ant}}} *$$

Hence, the equation for the antagonist–receptor complex is

$$\frac{d}{dt}\text{Ant-R}(t) = k_{on}^{\mathrm{Ant}} \cdot SF_{\mathrm{Ant}} \cdot \mathrm{R_{G,a}}(t) \cdot \mathrm{Ant_c}(t) - k_{off}^{\mathrm{Ant}} \cdot \text{Ant-R}(t) - k_{degr}^{\mathrm{Ant}} R \cdot \text{Ant-R}(t) \tag{41}$$

Due to the reversible binding, the modified equation for the central compartment becomes

$$\frac{d}{dt}\mathrm{Ant_c}(t) = k_A^{\mathrm{Ant}} \cdot \mathrm{Ant_d}(t) \cdot F^{\mathrm{Ant}}/V_c - cl^{\mathrm{Ant}} \cdot \mathrm{Ant_c}(t) - k_{cp}^{\mathrm{Ant}} \cdot \mathrm{Ant_c}(t) + k_{pc}^{\mathrm{Ant}} \cdot \mathrm{Ant_p}(t) - k_{on}^{\mathrm{Ant}} \cdot \mathrm{R_{G,a}}(t) \cdot \mathrm{Ant_c}(t) + k_{off}^{\mathrm{Ant}}/SF_{\mathrm{Ant}} \cdot \text{Ant-R}(t) \tag{39*}$$

The equation for active GnRH receptors in the presence of an antagonist is modified as follows:

$$\frac{d}{dt}\mathrm{R_{G,a}}(t) = k_{off}^{G} \cdot \text{G-R}(t) - k_{on}^{G} \cdot \mathrm{G}(t) \cdot \mathrm{R_{G,a}}(t) - k_{inter}^{\mathrm{R_G}} \cdot \mathrm{R_{G,a}}(t) + k_{recy}^{\mathrm{R_G}} \mathrm{R_{G,i}} - k_{on}^{\mathrm{Ant}} \cdot SF_{\mathrm{Ant}} \cdot \mathrm{Ant_c}(t) \cdot \mathrm{R_{G,a}}(t) + k_{off}^{\mathrm{Ant}} \cdot \text{Ant-R}(t) \tag{30**}$$

2.9. Simulation and parameter identification

The system of differential equations was solved numerically with LIMEX, a linearly implicit Euler method with extrapolation (Deuflhard and Nowak, 1987; Deuflhard et al., 1987). However, the main computational challenge is not to simulate the system, i.e. to solve the differential equations numerically, but to determine the unknown parameters in comparison with given data.

Our goal was to determine parameter values that minimize the difference between experimental measurement values and model predictions in a least-squares sense. The data sets are described in detail in Appendix D. From the scientific community's point of view, our model might be considered as being "over-parametrized". The authors do not very much like this wording because it does not relate to given data. The parameters chosen in the

Table 2
Receptor binding parameters for native GnRH, Nafarelin and Cetrorelix. The superscript letter "A" in the parameter names stands for the corresponding ligand Ago, Ant, or G (GnRH), respectively.

Parameter	k_{on}^{A}	k_{off}^{A}	$k_{degr}^{\mathrm{A\text{-}R}}$	$k_{diss}^{\mathrm{A\text{-}R}}$	k_{inact}^{A}	k_{act}^{A}
Unit	L/(d nmol)	1/d	1/d	1/d	1/d	1/d
Value	322.18	644.35	0.009	32.22	32.22	3.22

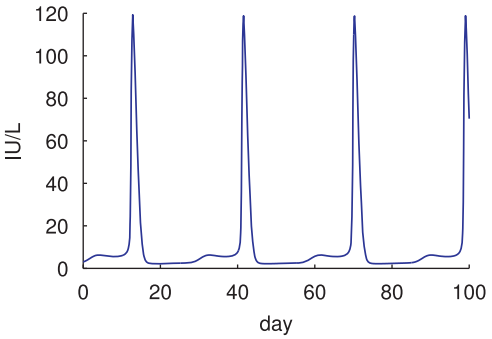

Fig. 5. Simulation result for LH in the time interval [0,100]. The model generates a periodic solution with cycle length of about 28 days.

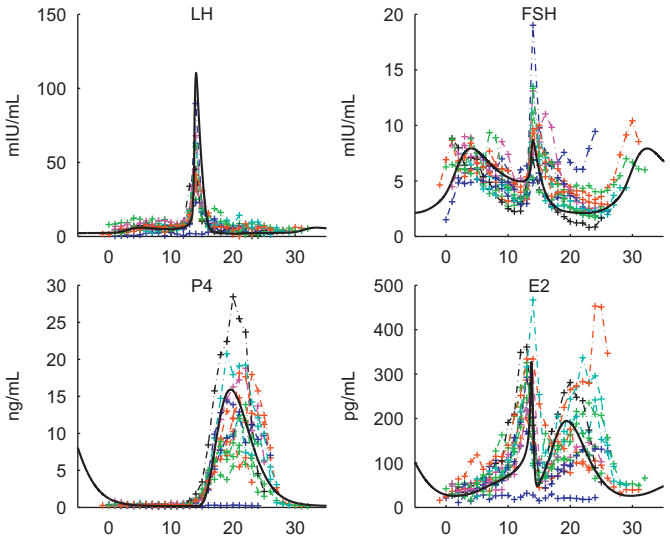

Fig. 6. Simulation results (solid lines) with parameters fitted to the data from 12 healthy women (LH, FSH, E2, P4). Individual patient level hormonal data were pulled from a Pfizer database. The time units are days.

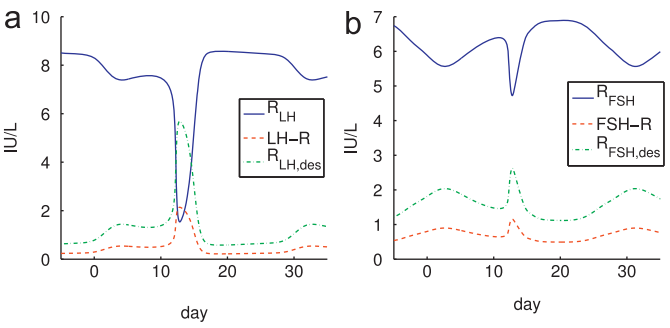

Fig. 7. Simulation result for the normal cycle: LH and FSH receptor binding.

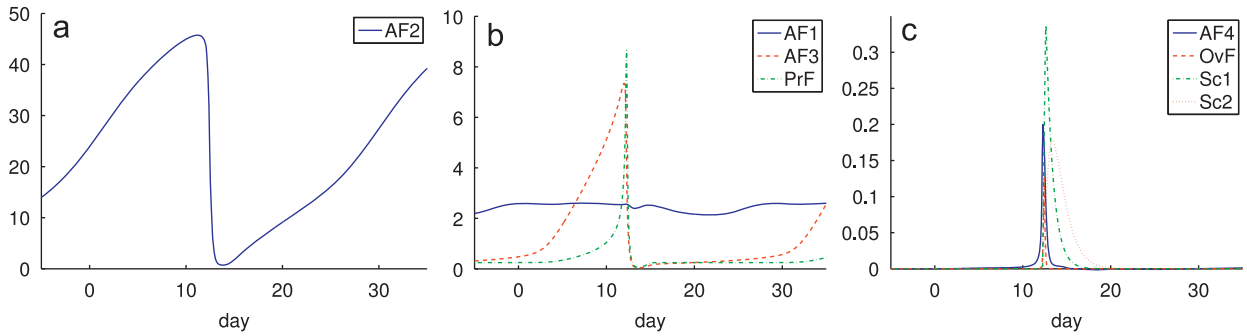

Fig. 8. Simulation result for the normal cycle: Follicular stages (arbitrary unit).

presented model are those that naturally arise in sub-models of mechanisms. Thus, they have a natural physical or chemical interpretation. Our Gauss–Newton method (Deuflhard, 2004) used for parameter estimation does split the parameter space into one part which can be identified by the given data, and another part which cannot. This splitting usually does not directly produce interpretable parameters. An improvement of the parameters can be achieved, if more data are available that contain information about the before unidentifiable parameter subspace. Many other optimization methods, when applied to nonlinear least-squares problems, e.g. the Levenberg–Marquardt algorithm, the Nelder–Mead algorithm (Matlab's *fminsearch*) or simulated annealing, to name just a few, ignore that fact because they do not take into account the structure of the "inverse" problem. These algorithms simply return a "solution" without additional information on identifiability or uniqueness. In contrast, the Gauss–Newton method applied by us monitors the numerical rank of the Jacobian and converges locally (for so-called adequate problems) to a solution that is unique within the subspace of identifiable parameters (Deuflhard, 2004). This method has been implemented in the code NLSCON (Nonlinear Least-Squares problems with CONstraints) (NLSCON), which is part of the software package PARKIN (PARameter identification in large KINetic networks) (Nowak and Deuflhard, 1985; Deuflhard and Nowak, 1986), and its recent update BioPARKIN (Dierkes et al., 2011). The latter one has been made publicly available at github[2] and used throughout this study.

Parameter identification has not been performed solely on the complete model, but has been used as a tool throughout the iterative process of successive model reduction and refinement. Some parameters could be identified in smaller sub-models, but became unidentifiable in the final closed-loop model. The sorting of the final 114 parameters according to their identifiability (see Table A1) refers to the complete model and depends on the specific parameter values, initial values and measurement time points.

First, we identified those parameters in model equations (1a)–(33) (model of the female menstrual cycle without administration of GnRH analogues) that could be estimated from the data of 12 healthy women with a normal menstrual cycle.[3] Since information on individual cycle length and day of last menses was missing, these data have been pooled according to the LH peak. However, we did not average the data. Instead, the individual data points were used for parameter estimation. We did not estimate individual parameters for every patient, but rather a set of average parameter values for the whole group of subjects, as in a multi-experiment setting (Deuflhard and Nowak, 1986). In the fully coupled model without GnRH analogue treatment, the number of identifiable parameters is 24 (out of 114), see Table A1. When the data for

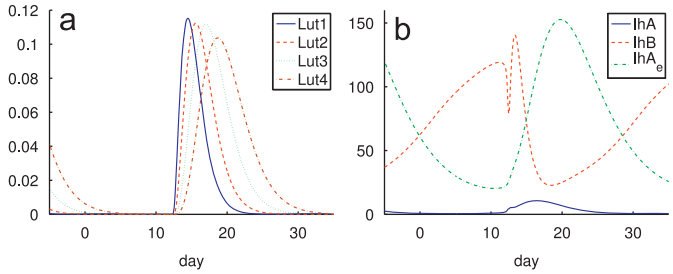

Fig. 9. Simulation result for the normal cycle: Development of corpus luteum (arbitrary unit), inhibin A, inhibin B, and effective inhibin A. Compared to inhibin A, effective inhibin A is delayed. Note that IhA and IhA$_e$ are measured in IU/mL, whereas IhB is measured in pg/mL.

Nafarelin and Cetrorelix administration were added, this number increased to 63.

For example, GnRH receptor binding parameters had to be re-estimated with GnRH analogue data because initially estimated values, which gave a good fit to normal cycle data, did not result in a good fit to GnRH analogue data. Literature on GnRH receptor binding rates is inconsistent, mainly because experimental conditions markedly vary (Bérault et al., 1983; Loumaye et al., 1984; Struthers et al., 2007; Sullivan et al., 2006). Sensitivity analysis revealed that the parameters $k_{degr}^{\text{Ago-R}}$, $k_{diss}^{\text{Ago-R}}$, k_{inact}^{Ago} and k_{act}^{Ago} are difficult to estimate, in contrast to k_{on}^{Ago} and k_{off}^{Ago}. Starting from values for native GnRH ($k_{on}^{G} = 2.5\ \text{nM}^{-1}\ \text{min}^{-1}$ and $k_{off}^{G} = 5\ \text{min}^{-1}$ as reported in Blum et al., 2000), we finally ended up with about ten times smaller values ($k_{on}^{\text{Ago}} \approx 0.25\ \text{nM}^{-1}\ \text{min}^{-1}$, $k_{off}^{\text{Ago}} \approx 0.5\ \text{min}^{-1}$), but the ratio $k_{off}/k_{on} = 2$ nM has been kept. The remaining parameters were determined such that the binding of native GnRH, Cetrorelix, and Nafarelin to GnRH receptors could be described with unified parameter values (Table 2).

The final set of parameter values (Table A1) was fixed for the simulation of the normal menstrual cycles as well as for the administration of GnRH analogues. Parameters have been estimated such that the cycle length in the simulation is about 28 days throughout. Initial values (Table B1) have been chosen in such a way that the simulation starts on a limit cycle.

3. Results and discussion

3.1. Normal cycles

The presented model generates a (quasi-)periodic solution[4] with cycle length of about 28 days, as illustrated by the LH

[2] https://github.com/CSB-at-ZIB/BioPARKIN

[3] Individual patient level hormonal data were pulled from a Pfizer database. The women were synchronized at the beginning of the study.

[4] Periodicity is not enforced mathematically.

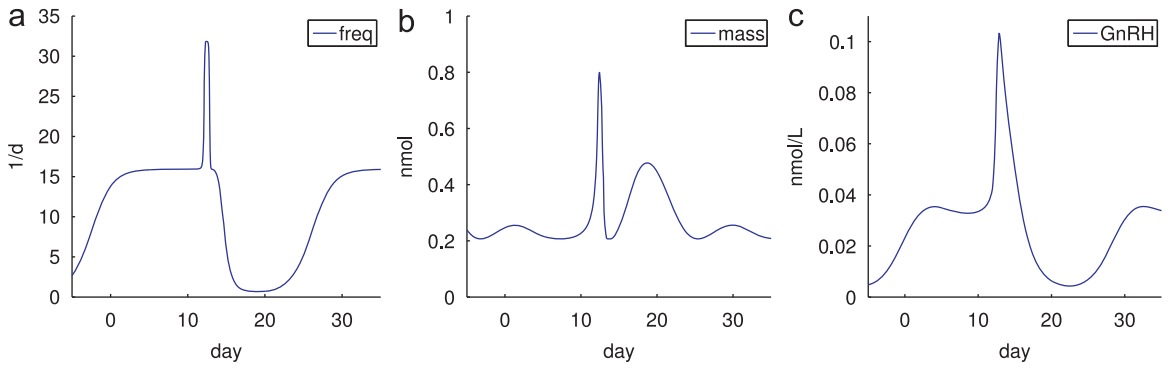

Fig. 10. Simulation result for the normal cycle: GnRH pulse frequency and mass, and GnRH.

pattern in Fig. 5. The simulation results in Fig. 6 show that the solution is consistent with the data for 12 healthy women with a normal menstrual cycle.

Besides the measured hormones, the simulations reveal the behavior of other model components, see Figs. 7–11. In particular, the results for GnRH pulse frequency agree with values reported in Chabbert-Buffet and Bouchard (2002) and Filicori et al. (1993): In the early follicular phase, peaks occur about every 90 min (frequency about 16/day). The frequency increases in the late follicular phase to about 24/day and attains its maximum (24-48/day) around the mid-cycle surge. In the luteal phase, the frequency slows down (about 2–6/day) and rapidly increases shortly before menses (8–12/day). Moreover, note that IhA_e attains its maximum 3 days later than IhA, thus accounting for a time-delay in the action of IhA.

3.2. GnRH Agonist Nafarelin

First, we studied the effect of *single* subcutaneous doses of Nafarelin (100 μg) at three different timepoints in the cycle: early follicular phase (cycle day 5), late follicular phase (cycle day 12), and luteal phase (cycle day 22). Data of three individual women were available from Monroe et al. (1985), one data set for each dosing regime. The three PK parameters V_c/F^{Ago}, k_A^{Ago} and cl^{Ago} were estimated individually for each of the three experiments (Tables 3 and 4).

The simulation results for LH are shown in Fig. 12. Administration of Nafarelin in the early follicular phase (Fig. 12(a)) postpones ovulation by 13 days (from day 13 to day 26), and this delay decreases with lower doses. This is in agreement with the experimental observations reported in the literature (Monroe et al., 1985) (ovulation about 15 days after administration, around cycle day 20, averaged over groups with doses of 1, 5, 20 and 100 μg between cycle days 3 and 6). As illustrated in Fig. 13, the agonist–receptor complex increases rapidly right after dosing, causing a sudden rise in LH, FSH, and E2. The LH and FSH peak re-initiate follicular development, thus postponing ovulation to a later point in time. The next LH peak on day 26 finally induces ovulation. Note that the absolute height of the LH peak is not important, as long as it occurs at the right time, i.e. when the preovulatory follicle is mature enough. Therefore, the small surge around day 26 is sufficient to cause ovulation, compare Fig. 13(f). GnRH receptors recover within 20 days (Fig. 13(e)), such that the post-treatment cycle is not altered.

Nafarelin administered in the late follicular phase immediately triggers ovulation (Fig. 12(b)), which explains its use for inducing oocyte maturation for in vitro fertilization (Fauser et al., 2002). The following cycles are slightly shortened, but they return to their original length (28 days) within 3 months. The cycle length is not altered when the dosing takes place 9 days after ovulation

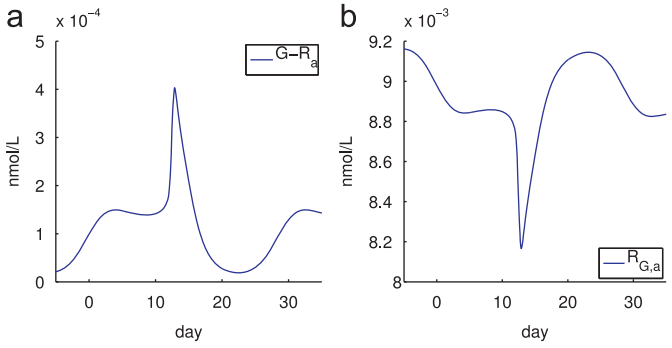

Fig. 11. Simulation result for the normal cycle: GnRH receptor complex and free GnRH receptors.

(Fig. 12(c)), but is shortened by 2 days with dosing 7 days after ovulation (results not shown). The authors in Monroe et al. (1985) report on a shortened cycle length if Nafarelin is administered at the end of the luteal phase but, again, this is an average over different doses and dosing days. Moreover, in agreement with Monroe et al. (1985) our simulations indicate that the luteal phase is truncated by Nafarelin administration (compare the P4 levels in Fig. 12(c)).

Furthermore, we studied the *multiple* dose administration of Nafarelin by intranasal spray (250 μg daily over 90 days). Data for one woman were available from Monroe et al. (1986). Since data for plasma drug concentrations are not available in this case, the parameters k_A^{Ago} and V_c/F^{Ago} were fixed as means of the single dose parameter values and only cl^{Ago} was estimated (Tables 3 and 4). The simulation results are presented in Fig. 14. After the initial stimulatory phase, LH and FSH levels are suppressed but acute responses to Nafarelin are maintained. Our results agree with Monroe et al. (1986), where the authors report on basal E2 levels of 25 pg/mL and a reduce of peak LH responses by 70%. In all cases, ovulation is inhibited (absence of luteal phase). The acute E2 response is still evident, but the higher the dose, the more profound the suppression of E2 (figures not shown). This is in line with observations in Monroe et al. (1986). Note that chronically diminished E2 levels can lead to osteoporosis, which precludes longer agonist treatment. The simulations also show that desensitization goes along with a depletion of the gonadotropin pools in the pituitary (Fig. 14(f)) and moderate receptor downregulation (Fig. 14(e)). It takes about eight cycles to regain pre-treatment hormone and receptor levels. Nevertheless, ovulatory menstrual function returns rapidly after treatment.

3.3. GnRH antagonist Cetrorelix

Simulations for single dose administration of Cetrorelix were performed with different doses D_{Ant} and different times of dosing

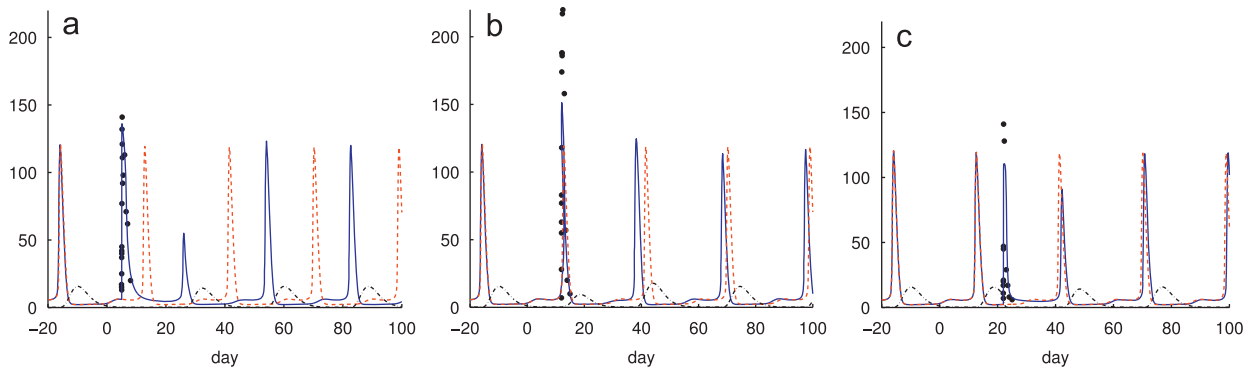

Fig. 12. Simulation results for LH (solid blue curve) for the administration of 100 μg Nafarelin (single dose) at different times in the cycle (data from Monroe et al., 1985). The dashed red curve represents the solution for LH without dosing. Administration in the early follicular phase delays ovulation, administration in the late follicular phase immediately causes ovulation, and administration in the luteal phase leads to a truncated luteal phase. P4 is represented by dash-dotted black lines. The unit of the *y*-axis is ng/mL for P4 and mIU/mL for LH. (a) Early follicular phase (day 5). (b) Late follicular phase (day 12). (c) Luteal phase (day 22). (For interpretation of the references to color in this figure legend, the reader is referred to the web version of this article.)

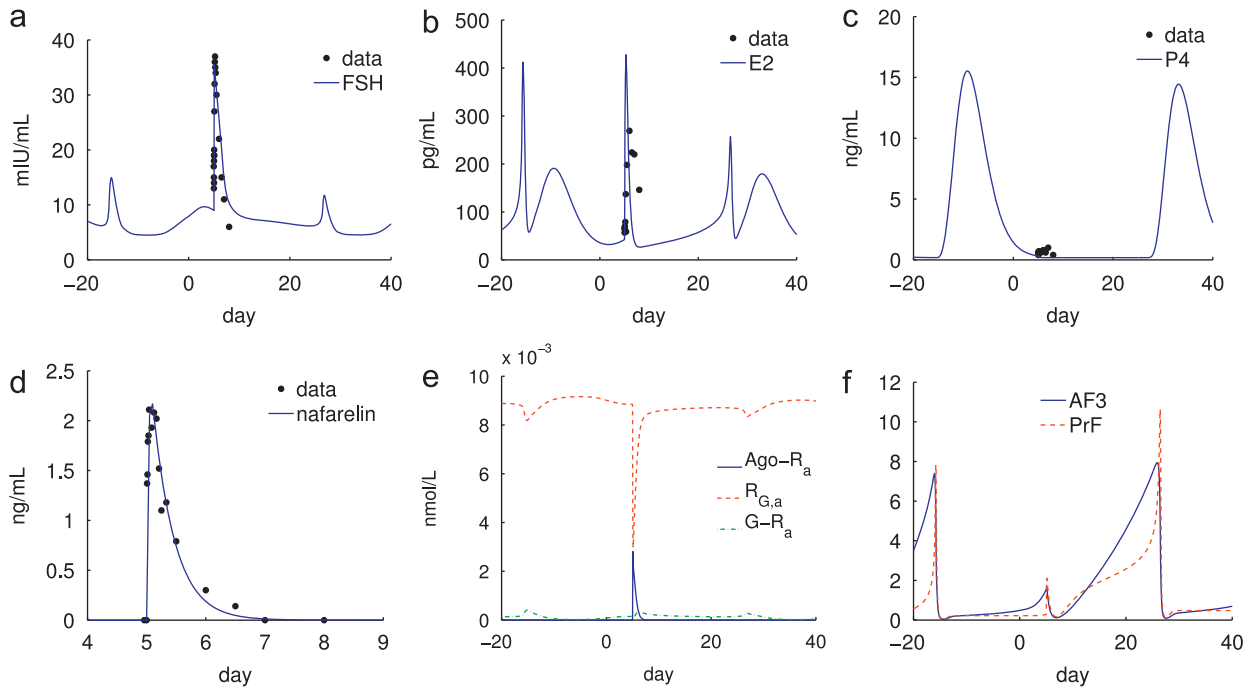

Fig. 13. Simulation results for the administration of 100 μg Nafarelin (single dose) in the early follicular phase (day 5). (a) FSH; (b) E2; (c) P4; (d) Nafarelin; (e) receptor complex; and (f) Follicles (arbitrary unit).

as reported in Leroy et al. (1994), Duijkers et al. (1998). Due to the heterogeneity of results published in the literature, we also kept the receptor binding parameter values of GnRH for the simulations with Cetrorelix (Table 2). The clearance rate constant cl^{Ant} was adjusted to fit different data sets, see Table 4. All other parameter values were kept fixed.

First we studied the *single* s.c. administration of Cetrorelix (0.25 mg, 0.5 mg, and 1 mg) in the *early* follicular phase (cycle day 3). Median data (LH, FSH, E2, and Cetrorelix) from groups of 12 patients have been published by Duijkers et al. (1998). Individual data were not accessible, but a PK/PD model for these (unpublished) data was developed by Nagaraja et al. (2003). We therefore used their parameter values (Table 3) for our simulations.

Simulation results for the administration of 0.5 mg are shown in Fig. 15. Note that the peak hormone concentrations at ovulation do not show up in the median data due to averaging. LH, FSH, and E2 concentrations decrease immediately after dosing, exactly as reported in Duijkers et al. (1998). The reason is a decrease in the number of free GnRH receptors (Fig. 15(f)) and thus in the GnRH-receptor complex (Fig. 15(e)) due to competitive binding to Cetrorelix. Thus, LH and FSH release is inhibited. Moreover, our simulation results are in line with the observation in Duijkers et al. (1998) that the administration does not result in an apparent delay of ovulation. The short-term decrease of LH and FSH after dosing results in a decrease of the corresponding receptor complexes (figures not shown), but the concentrations still remain high enough for normal follicular maturation. We repeated the simulations with smaller (0.25 mg) and higher (1 mg, 5 mg) doses and concluded that these effects are dose-independent (results not shown).

Individual patient data (LH, E2, P4) for single dose administration of Cetrorelix (5 or 3 mg) in the *late* follicular phase have been published by Leroy et al. (1994). Since plasma Cetrorelix concentrations are missing in these data, we decided to use the same PK parameters as for the Duijkers data. The simulation results are illustrated in Fig. 16. Similar to the lower doses (≤ 1 mg) in the early follicular phase, LH and E2 concentrations decrease immediately after dosing. In contrast to the early follicular phase, dosing in

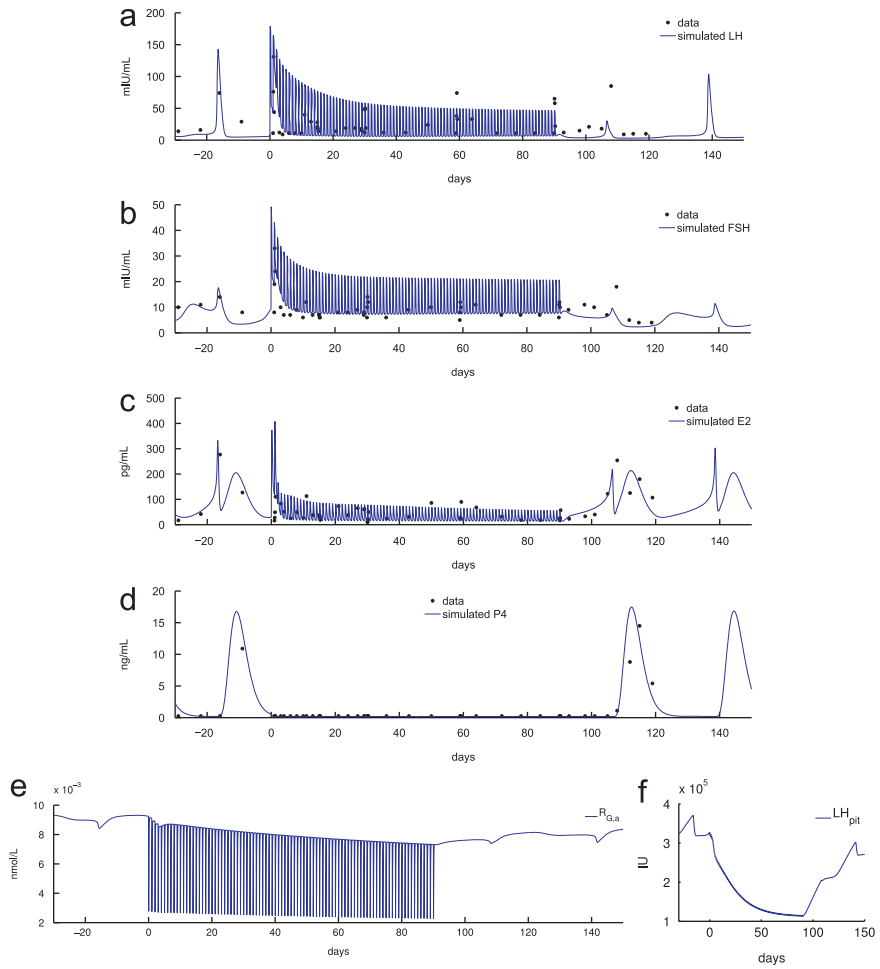

Fig. 14. Simulation results for the daily administration of 250 μg Nafarelin on cycle days 1–90 (individual data from Jaffe et al., 1986, also published and discussed in Monroe et al., 1986). After an initial stimulatory phase, LH, FSH and E2 levels are suppressed but acute responses to Nafarelin are maintained, whereas P4 is suppressed constantly. (a) LH; (b) FSH; (c) E2; (d) P4; (e) GnRH receptors and (f) LH in the pituitary.

the late follicular phase postpones ovulation, which agrees with published data (Leroy et al., 1994). This ability to prevent premature LH surges makes GnRH antagonists useful for IVF treatment. The extent of this delay, however, seems to be patient-specific rather than dose-dependent. In our model, the length of the suppressive effect depends on the individual clearance rate of Cetrorelix from the central compartment. This might explain the difficulty in predicting individual pattern of response and the occasional need for additional doses a few days after the first dose (Olivennes et al., 2000). Our simulation results also support the assumption that the follicles tolerate the temporary withdrawal of gonadotropins and E2 during the follicular phase, and that they resume their original function after treatment.

We also studied the *multiple* dose administration of Cetrorelix (0.25 mg, 0.5 mg, or 1 mg) between cycle days 3 and 16. Again, median data (LH, FSH, E2, and Cetrorelix) for groups of 12 patients have been published by Duijkers et al. (1998). The time point of ovulation after the final dose is hardly visible in the data because hormonal peaks disappeared by data averaging. Since individual data were not accessible, we again used the PK parameters from Nagaraja et al. (2003).

In our simulations (Fig. 17), ovulation is delayed by 7 days (0.25 mg), 9.5 days (5 mg), or 11.5 days (1 mg), respectively, which agrees quite well with the dose-dependent median delays reported in Duijkers et al. (1998) (5, 10 and 13 days in the 0.25, 0.5, and 1 mg dose groups). An acute response to Cetrorelix is visible for all doses in all measured components (LH, FSH, and E2), but median values are suppressed over treatment (Fig. 18), and the suppression gets stronger with increasing dose (results not shown). The simulations show that desensitization does not go along with a depletion of gonadotropin pools, in contrast to the long-term agonist protocol (compare Fig. 18(e) and Fig. 14(f)). The average number of free GnRH receptors and thus the GnRH receptor-complex decrease slightly over the treatment period (Fig. 18(d)). However, the receptors recover within a few days after the final dose such that luteal function is normal, and the next cycle after treatment has length of 28 days.

Table 3
Pharmacokinetic parameters for single dose Nafarelin administration (estimated from individual patient data) and for the administration of single (sd) and multiple dose (md) Cetrorelix (group average parameters from Nagaraja et al., 2003). The superscript letter "A" in the parameter names stands for Ant or Ago, respectively.

Parameter	V_c/F^A	k_A^A	k_{cp}^A	k_{pc}^A
Unit	L	1/d	1/d	1/d
Nafarelin sd (day 5)	38.12	71.68	–	–
Nafarelin sd (day 12)	28.34	87.32	–	–
Nafarelin sd (day 22)	21.57	62.06	–	–
Nafarelin md	29.34	73.69	–	–
Cetrorelix sd (group average)	34.90	65.2	3.216	4.76
Cetrorelix md (group average)	43.03	73.84	2.704	0.396

3.4. Summary

Simulation results for single and multiple dosing of Nafarelin and Cetrorelix are in good qualitative agreement with the data. Better quantitative agreement might be achieved with more intensive sampling of multiple hormones during the complete cycle. In addition, the data for the dosing event should ideally come along with measurements that were taken during the non-treatment cycle. This kind of data would allow for an individual parametrization of both the non-treatment and the treatment cycle, including individual cycle length and basal hormone levels. In this case, a better fit to individual dosing data would be obtained. For the available data, this could not be achieved, since the different data sets originated from different studies and thus different groups of patients. Hence we could only build an average model based on averaged data.

Table 4
Parameters for the administration of single dose (sd) and multiple dose (md) Nafarelin or Cetrorelix. d_0 denotes the first day of dosing, d_f the last day. The dose is denoted by D_A. The parameter cl^A for clearance from the central compartment turned out to be the most sensitive and best identifiable parameter and was therefore varied between the different data sets.

Parameter	d_0	d_f	D_A	cl^A
Unit	d	d	μg	1/d
Nafarelin sd (day 5)	5	5	100	2.65
Nafarelin sd (day 12)	12	12	100	6.85
Nafarelin sd (day 22)	22	22	100	4.84
Nafarelin md	1	90	250	20.0
Cetrorelix sd (1)	0	0	5000	1.0
Cetrorelix sd (2)	0	0	5000	0.6
Cetrorelix sd (3)	0	0	5000	5.0
Cetrorelix sd (4)	0	0	3000	1.8
Cetrorelix sd (0.25 mg)	3	3	250	6.0
Cetrorelix sd (0.5 mg)	3	3	500	5.0
Cetrorelix sd (1 mg)	3	3	1000	5.0
Cetrorelix md (0.25 mg)	3	16	250	3.0
Cetrorelix md (0.5 mg)	3	16	500	3.0
Cetrorelix md (1 mg)	3	16	1000	3.0

Parameter identification gets difficult or even impossible with averaged data when averaging takes place for women with different cycle lengths and/or at different phases of the cycle as for example in Duijkers et al. (1998). The reason is that such data can simply not be explained by a single parametrization. For mathematical modeling, individual data are clearly preferable. Nevertheless, the number of identifiable parameters increased significantly when Nafarelin and Cetrorelix data were included.

Our model emphasizes the importance of the times of dosing during the cycle, and it gives insight into the recovery of the cycle after the final dose. The model is robust in the sense that, after the final dose, the solution returns to the initial limit cycle. Beyond the results given here, a different parametrization would lead to a destabilization of the cycle, which might be an interesting topic for further investigations. The simulation results indicate that the recovery process of GnRH receptors after long-term antagonist treatment (Fig. 18(d)) is faster compared to agonist treatment (Fig. 14(e)), but a detailed analysis remains to be done.

Depending on the presumed usage of the model, more levels of detail might be added to the model. For example, if one is interested in the pulsatile pattern of GnRH and LH, models for the GnRH pulse generator (Brown et al., 1994; Keenan et al., 2000; Vidal and Clément, 2010) can be coupled to the presented model. As a future challenge, it also remains to include more knowledge about the effect of GnRH on its target pituitary cells (Lim et al., 2009; Tsaneva-Atanasova1 et al., 2012) into the model. New approaches will be needed to deal with such multi-scale problems.

Due to the subtle interference of model refinement and data availability, we clearly want our model to be understood as a starting point for further investigations.

4. Conclusion

The mathematical model developed in this paper describes the hormone profiles throughout the female menstrual cycle in correspondence with measurement values of LH, FSH, P4 and E2 for 12 individual healthy women. A key step for simulating the administration of GnRH analogues was the elimination of time delays and

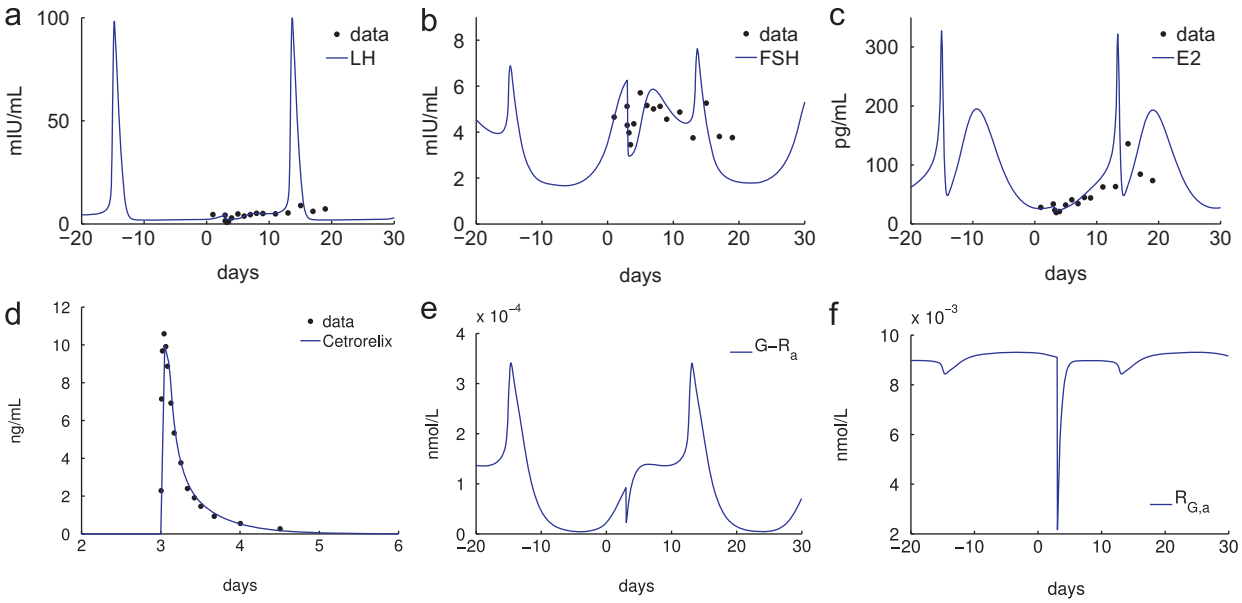

Fig. 15. Simulation results (solid blue curve) and data (black dots, median for $n=12$, from Duijkers et al. (1998)) following single s.c. administration of 0.5 mg Cetrorelix in the *early* follicular phase (cycle day 3). As expected, the administration does not result in an apparent delay of ovulation. (For interpretation of the references to color in this figure legend, the reader is referred to the web version of this article.)

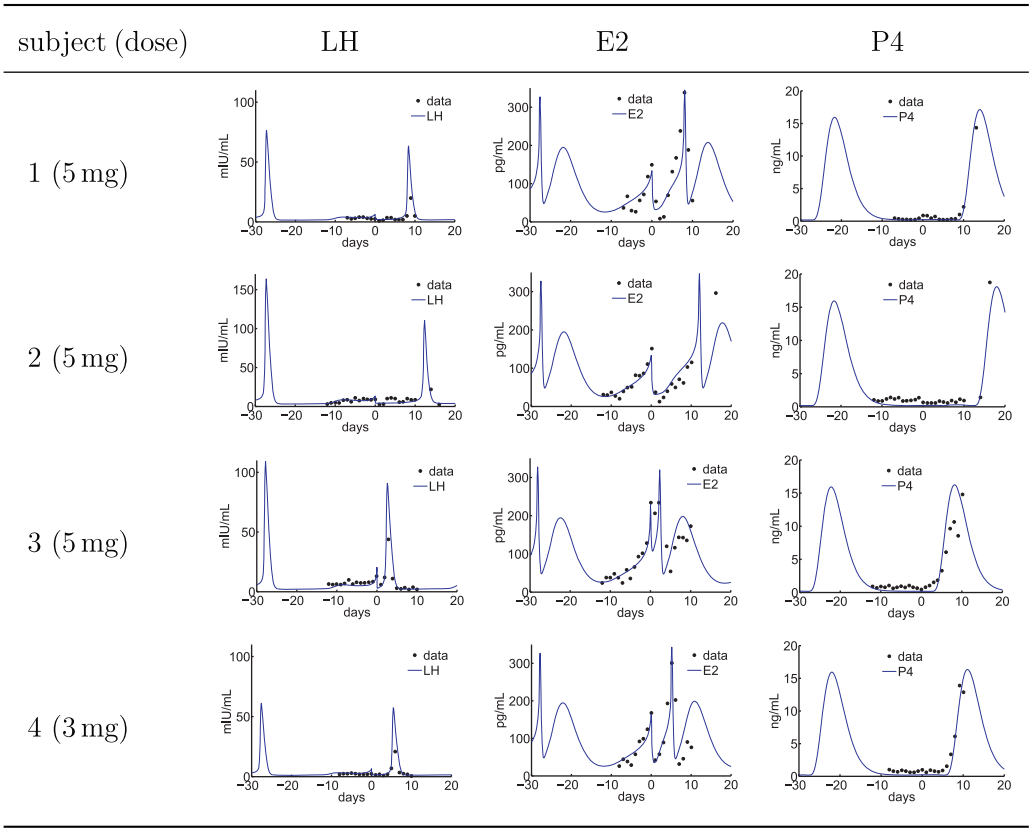

Fig. 16. Simulation results (solid blue curve) and data (black dots, from Leroy et al., 1994) of four representative women following single s.c. administration of 5 mg or 3 mg Cetrorelix in the *late* follicular phase. The LH peak occurs 9, 14, 3 or 5 days after antagonist administration, depending on the individual degradation rate of Cetrorelix. (For interpretation of the references to color in this figure legend, the reader is referred to the web version of this article.)

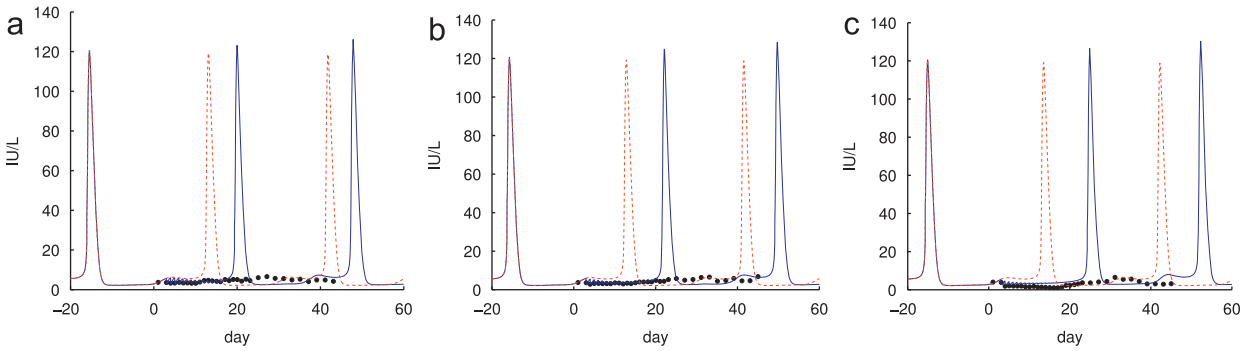

Fig. 17. Simulation results for LH (solid blue curve) and data (black dots, median for $n=12$ per group, from Duijkers et al., 1998) following daily administration of Cetrorelix between cycle days 3 and 16. The dashed red curve represents the solution without dosing. Note that the averaging of individual data led to a loss of the LH peaks in the data points. Nevertheless, in agreement with results reported in literature, ovulation is delayed by 7 days (0.25 mg), 9.5 days (0.5 mg), or 11.5 days (1 mg), respectively. (a) 0.25 mg; (b) 0.5 mg; and (c) 1 mg. (For interpretation of the references to color in this figure legend, the reader is referred to the web version of this article.)

the integration of a deterministic model for the GnRH pulse pattern. The deterministic modeling turned out to be fully sufficient for our purposes. Unlike previous models (Harris, 2001; Reinecke and Deuflhard, 2007; Pasteur, 2008), the new model correctly predicts the changes in the cycle following single and multiple dose administration of a GnRH agonist or antagonist at different stages in the cycle. To the best of our knowledge, this is the first mathematical model that describes such feedback mechanisms in consideration of cyclicity of the female hormonal balance.

The model applied herein for the normal cycle without GnRH analogues comprises 33 differential equations and 114 unknown parameters. Twenty-four parameters could be identified from the data of 12 individual women. The number of identifiable parameters increased to 63 when Nafarelin and Cetrorelix data were included. Thus, we have learned more about the system by studying the effect of pharmacological intervention. Our objective for the future is to not just model the virtual cycle of an "idealized woman", but to describe individual patients by reliable individual models.

Quantitative Systems Pharmacology (QSP) is an emerging concept and consensus on its exact definition is still evolving (van der Graaf, 2012). Although we believe that the mathematical model presented in this paper contains some mechanistic elements and multi-scale features in line with a QSP approach (Ward, 2011), in its present form it can only be seen and utilized as a semi-mechanistic PK/PD model and a first step towards a full-scale QSP framework of the menstrual cycle. From a drug discovery and development perspective, the justification of the

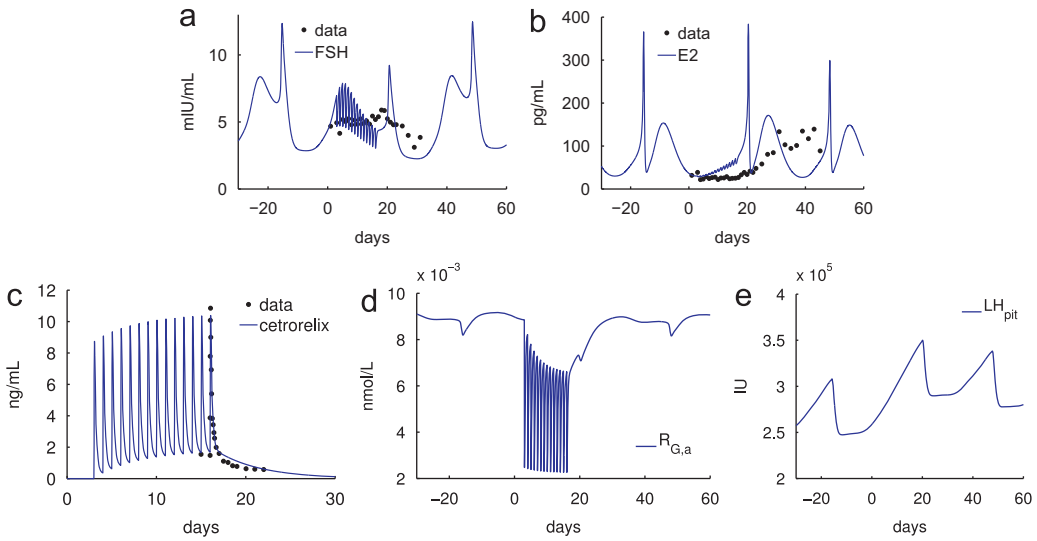

Fig. 18. Simulation results (blue solid curve) and data (black dots, median for $n=12$, from Duijkers et al., 1998) following daily administration of 0.5 mg Cetrorelix between cycle days 3 and 16. Ovulation is delayed by 13 days. Note that the averaging of individual data led to a loss of the hormonal peaks. (a) FSH; (b) E2; (c) Cetrorelix; (d) GnRH receptors; and (e) GnRH receptors. (For interpretation of the references to color in this figure legend, the reader is referred to the web version of this article.)

extent of further investments in such a QSP approach would come from a clear definition of the key questions and issues that cannot be addressed by simpler, fit-for-purpose models. There is need and an opportunity for (precompetitive) collaboration in this area across industry, academia and regulatory agencies through which data can be shared to facilitate model validation and further development.

Appendix A. Parameter values

Parameter values are listed in Table A1.

Appendix B. Initial values

Initial values are listed in Table B1.

Appendix C. Conversion of units

The presented model equations are consistent with respect to physical units. Since we wanted the units of the output curves for measured quantities to agree with the (inconsistent) units of the corresponding measurement values, we introduced correction factors SF_{Ago} and SF_{Ant} in the model equations to account for the conversion of units. These factors were computed from the molar weights

$$M_{\mathrm{Naf}} = 1322.49\ \mathrm{g/mol}, \quad M_{\mathrm{Cet}} = 1431.06\ \mathrm{g/mol}.$$

Since Nafarelin is measured in ng/mL ($1\ \mathrm{ng/mL} = 10^{-6}\ \mathrm{g/L} \equiv 10^{-6}\ \mathrm{(g/L)}/1322.49\ \mathrm{(g/mol)} = 0.7561\ \mathrm{nmol/L}$), we decided for nmol/L as unit for the unknown quantities (receptors, receptor complexes). The conversion of units for Cetrorelix conforms to $1\ \mathrm{ng/mL} \equiv 10^{-6}\ \mathrm{(g/L)}/1431.06\ \mathrm{(g/mol)} = 0.6988\ \mathrm{nmol/L}$. Thus

$$SF_{\mathrm{Ago}} = 0.7561\ \mathrm{ng/pmol}, \quad SF_{\mathrm{Ant}} = 0.6988\ \mathrm{ng/pmol}.$$

The physical units of all system components are listed in Table B1.

Appendix D. Data sources

In the following, we cite the publications wherefrom data for single and multiple dose administration of Nafarelin and Cetrorelix have been taken.

D.1. Single dose Nafarelin

Citation from Monroe et al. (1985): The study was conducted with 28 healthy women (age 22 to 46, normal ovulatory function). Nafarelin was provided in a 0.9% solution of sodium chloride and was administered in single doses of 1, 5, 20, and 100 μg. The solution was injected subcutaneously (1.0 mL) into the individual subjects during one of the three physiological phases of the menstrual cycle. Eleven women received the GnRH agonist during the early follicular phase, 3–6 days after the onset of menstruation (1 μg, $n=3$; 5 μg, $n=3$; 20 μg, $n=1$; 100 μg, $n=4$). Eight women received the medication in the late follicular phase on days 10–13 of the menstrual cycle (1 μg, $n=3$; 5 μg, $n=3$; 100 μg, $n=2$). The nine remaining volunteers were treated in the luteal phase, 1 to 10 days after presumed ovulation (1 μg, $n=2$; 5 μg, $n=3$; 20 μg, $n=1$; 100 μg, $n=3$). Throughout each treatment cycle, blood samples were taken every other day for the first 10 days and daily for the next 7 days. Thereafter, blood sampling was performed every other day until the start of the next menstrual period. Blood sampling also was performed at −60, −30, 0 (immediately before administration), +10, 20, 30, 45, and 60 min, and 2, 4, 6, 8, 12, 24, 36, 48, and 72 h after the injection. Serum was frozen for later measurement of LH, FSH, E2, P4, and Nafarelin. Nafarelin administration during the early follicular phase delayed ovulation by 4.6 ± 1.7 days (ovulation occurred about 15 days after administration, on or around cycle day 20) and prolonged the duration of the menstrual cycle by about 4 days compared to the pretreatment cycle. When Nafarelin was administered shortly before or after ovulation, cycle length was not altered consistently (shorted by 2.3 ± 1 days, but statistically not significant). Administration 7–10 days after ovulation resulted in a truncated luteal phase and shortened cycle length (about 4 days).

D.2. Multiple dose Nafarelin

Citation from Monroe et al. (1986): 32 women with ovulatory menstrual cycles were given 125 μg (group 1), 250 μg (group 2),

Table A1
Parameter values (d=days). A double star behind the parameter number indicates parameters that could be identified from normal cycle data, whereas a single star marks parameters that could be identified by additionally including the data for GnRH analogue treatment.

No.	Symbol	Value	Unit
1*	b_{Syn}^{LH}	7309.92	IU/d
2	k_{E2}^{LH}	7309.92	IU/d
3	T_{E2}^{LH}	192.2	pg/mL
4	n_{E2}^{LH}	10	–
5	T_{P4}^{LH}	2.371	ng/mL
6	n_{P4}^{LH}	1	–
7*	b_{Rel}^{LH}	0.00476	1/d
8*	$k_{G\text{-}R}^{LH}$	0.1904	1/d
9**	$T_{G\text{-}R}^{LH}$	0.0003	nmol/L
10**	$n_{G\text{-}R}^{LH}$	5	–
11**	V_{blood}	6.589	L
12*	k_{on}^{LH}	2.143	L/(d IU)
13*	k_{cl}^{LH}	74.851	1/d
14*	k_{recy}^{LH}	68.949	1/d
15*	k_{des}^{LH}	183.36	1/d
16**	T_{freq}^{FSH}	12.8	1/d
17	n_{freq}^{FSH}	5	–
18*	k_{lh}^{FSH}	2.213e+4	IU/d
19**	$T_{lh}A$	95.81	IU/mL
20	$T_{lh}B$	70	pg/mL
21	$n_{lh}A$	5	–
22	$n_{lh}B$	2	–
23*	b_{Rel}^{FSH}	0.057	1/d
24*	$k_{G\text{-}R}^{FSH}$	0.272	1/d
25*	$T_{G\text{-}R}^{FSH}$	0.0003	nmol/L
26**	$n_{G\text{-}R}^{FSH}$	2	–
27	k_{on}^{FSH}	3.529	L/(d IU)
28*	k_{cl}^{FSH}	114.25	1/d
29	k_{recy}^{FSH}	61.029	1/d
30*	k_{des}^{FSH}	138.3	1/d
31	T_{FSH}^{s}	3	IU/L
32	n_{FSH}^{s}	5	–
33	T_{P4}^{s}	1.235	ng/mL
34	n_{P4}^{s}	5	–
35*	k^{s}	0.219	1/d
36	k_{cl}^{s}	1.343	1/d
37	$n_{FSH\text{-}R}^{AF1}$	5	–
38*	$T_{FSH\text{-}R}^{AF1}$	0.608	IU/L
39	k^{AF1}	3.662	[PrA1]/d
40	k_{AF1}^{AF2}	1.221	L/(d IU)
41**	$SF_{LH}R$	2.726	IU/L
42*	k_{AF2}^{AF3}	4.882	1/d
43**	n_{AF2}^{AF3}	3.689	–
44*	k_{AF3}^{AF3}	0.122	L/(d IU)
45	SeF_{max}	10	[SeF1]
46*	k_{AF3}^{AF4}	122.06	1/d
47*	n_{AF3}^{AF4}	5	–
48*	k_{AF4}^{AF4}	12.206	1/d
49	n^{AF4}	2	–
50*	k_{AF4}^{PrF}	332.75	1/d
51	k_{cl}^{PrF}	122.06	1/d
52	n^{OvF}	6	–
53	k^{OvF}	7.984	1/d
54	T_{PrF}^{OvF}	3	[PrF]
55	n_{PrF}^{OvF}	10	–
56	k_{cl}^{OvF}	12.206	1/d
57**	k^{Sc1}	1.208	1/d
58	T_{OvF}^{Sc1}	0.02	[OvF]
59	n_{OvF}^{Sc1}	10	–
60	k_{Sc1}^{Sc2}	1.221	1/d
61*	k_{Sc2}^{Lut1}	0.958	1/d
62	k_{Lut1}^{Lut2}	0.925	1/d

Table A1 (*continued*)

No.	Symbol	Value	Unit
63	$k_{\mathrm{Lut2}}^{\mathrm{Lut3}}$	0.7567	1/d
64*	$k_{\mathrm{Lut3}}^{\mathrm{Lut4}}$	0.610	1/d
65**	k_{cl}^{Lut4}	0.543	1/d
66*	$m_{\mathrm{G\text{-}R}}^{\mathrm{Lut}}$	20	–
67*	$T_{\mathrm{G\text{-}R}}^{\mathrm{Lut}}$	0.0008	nmol/L
68*	$n_{\mathrm{G\text{-}R}}^{\mathrm{Lut}}$	5	–
69*	b^{E2}	51.558	$\frac{\mathrm{pg/mL}}{\mathrm{d}}$
70*	$k_{\mathrm{AF2}}^{\mathrm{E2}}$	2.0945	$\frac{\mathrm{pg/mL}}{\mathrm{[AF2]\ d}}$
71*	$k_{\mathrm{AF3}}^{\mathrm{E2}}$	9.28	$\frac{\mathrm{pg/mL}}{\mathrm{[AF3]\ [LH]\ d}}$
72*	$k_{\mathrm{AF4}}^{\mathrm{E2}}$	6960.53	$\frac{\mathrm{pg/mL}}{\mathrm{[AF4]\ d}}$
73	$k_{\mathrm{PrF}}^{\mathrm{E2}}$	0.972	$\frac{\mathrm{pg/mL}}{\mathrm{[PrF]\ [LH]\ d}}$
74*	$k_{\mathrm{Lut1}}^{\mathrm{E2}}$	1713.71	$\frac{\mathrm{pg/mL}}{\mathrm{[Lut1]\ d}}$
75**	$k_{\mathrm{Lut4}}^{\mathrm{E2}}$	8675.14	$\frac{\mathrm{pg/mL}}{\mathrm{[Lut4]\ d}}$
76**	k_{cl}^{E2}	5.235	1/d
77*	b^{P4}	0.943	$\frac{\mathrm{ng/mL}}{\mathrm{d}}$
78**	$k_{\mathrm{Lut4}}^{\mathrm{P4}}$	761.64	$\frac{\mathrm{ng/mL}}{\mathrm{[Lut4]\ d}}$
79*	k_{cl}^{P4}	5.13	1/d
80	b^{IhA}	1.445	$\frac{\mathrm{IU/mL}}{\mathrm{d}}$
81	$k_{\mathrm{PrF}}^{\mathrm{IhA}}$	2.285	$\frac{\mathrm{IU/mL}}{\mathrm{[PrF]\ d}}$
82	$k_{\mathrm{Sc1}}^{\mathrm{IhA}}$	60	$\frac{\mathrm{pg/mL}}{\mathrm{[Sc1]\ d}}$
83	$k_{\mathrm{Lut1}}^{\mathrm{IhA}}$	180	$\frac{\mathrm{pg/mL}}{\mathrm{[Lut1]\ d}}$
84	$k_{\mathrm{Lut2}}^{\mathrm{IhA}}$	28.211	$\frac{\mathrm{IU/mL}}{\mathrm{[Lut2]\ d}}$
85	$k_{\mathrm{Lut3}}^{\mathrm{IhA}}$	216.85	$\frac{\mathrm{IU/mL}}{\mathrm{[Lut3]\ d}}$
86	$k_{\mathrm{Lut4}}^{\mathrm{IhA}}$	114.25	$\frac{\mathrm{IU/mL}}{\mathrm{[Lut4]\ d}}$
87	k^{IhA}	4.287	1/d
88**	$k_{cl}^{\mathrm{IhA_e}}$	0.199	1/d
89	b^{IhB}	89.493	$\frac{\mathrm{pg/mL}}{\mathrm{d}}$
90	$k_{\mathrm{AF2}}^{\mathrm{IhB}}$	447.47	$\frac{\mathrm{pg/mL}}{\mathrm{[AF2]\ d}}$
91	$k_{\mathrm{Sc2}}^{\mathrm{IhB}}$	134240.2	$\frac{\mathrm{pg/mL}}{\mathrm{[AF3]\ d}}$
92	k_{cl}^{IhB}	172.45	1/d
93	f_0	16	1/d
94*	$T_{\mathrm{P4}}^{\mathrm{freq}}$	1.2	ng/mL
95	$n_{\mathrm{P4}}^{\mathrm{freq}}$	2	–
96	$m_{\mathrm{E2}}^{\mathrm{freq}}$	1	–
97*	$T_{\mathrm{E2}}^{\mathrm{freq}}$	220	pg/mL
98	$n_{\mathrm{E2}}^{\mathrm{freq}}$	10	–
99**	a_0	$5.593\mathrm{e}-3$	nmol
100**	$T_{\mathrm{E2}}^{\mathrm{mass,1}}$	220	pg/mL
101*	$n_{\mathrm{E2}}^{\mathrm{mass,1}}$	2	–
102**	$T_{\mathrm{E2}}^{\mathrm{mass,2}}$	9.6	pg/mL
103**	$n_{\mathrm{E2}}^{\mathrm{mass,2}}$	1	–
104**	k_{degr}^{G}	0.447	1/d
105**	k_{on}^{G}	322.18	$\frac{\mathrm{L}}{\mathrm{d\ nmol}}$
106**	k_{off}^{G}	644.35	1/d
107**	$k_{degr}^{\mathrm{G\text{-}R}_i}$	0.00895	1/d
108	$k_{diss}^{\mathrm{G\text{-}R}_i}$	32.218	1/d
109*	$k_{inter}^{\mathrm{R_G}}$	3.222	1/d
110*	$k_{recy}^{\mathrm{R_G}}$	32.218	1/d
111**	$k_{degr}^{\mathrm{R_G}}$	0.0895	1/d
112*	$k_{inact}^{\mathrm{G\text{-}R}}$	32.218	1/d

Table A1 (*continued*)

No.	Symbol	Value	Unit
113	$k_{act}^{G\text{-}R}$	3.222	1/d
114**	$k_{syn}^{R_G}$	8.949e−5	$\frac{\text{nmol}}{\text{L d}}$

Table B1
Initial values.

No.	Component	Value	Unit
1	LH_{pit}	3.141e+5	IU
2	LH_{blood}	3.487	IU/L
3	R_{LH}	8.157	IU/L
4	LH-R	0.332	IU/L
5	$R_{LH,des}$	0.882	IU/L
6	FSH_{pit}	6.928e+4	IU
7	FSH_{blood}	6.286	IU/L
8	R_{FSH}	5.141	IU/L
9	FSH-R	1.030	IU/L
10	$R_{FSH,des}$	2.330	IU/L
11	s	0.417	–
12	AF1	2.811	[Foll]
13	AF2	27.64	[Foll]
14	AF3	0.801	[Foll]
15	AF4	6.345e−5	[Foll]
16	PrF	0.336	[Foll]
17	OvF	1.313e−16	[Foll]
18	Sc1	1.433e−10	[Foll]
19	Sc2	7.278e−8	[Foll]
20	Lut1	1.293e−6	[Foll]
21	Lut2	3.093e−5	[Foll]
22	Lut3	4.853e−4	[Foll]
23	Lut4	3.103e−3	[Foll]
24	E2	30.94	pg/mL
25	P4	0.688	ng/mL
26	IhA	0.637	IU/mL
27	IhB	72.17	pg/mL
28	IhA_e	52.43	IU/mL
29	G	1.976e−2	nmol/L
30	$R_{G,a}$	9.121e−3	nmol/L
31	$R_{G,i}$	9.893e−4	nmol/L
32	$G\text{-}R_a$	8.618e−5	nmol/L
33	$G\text{-}R_i$	7.768e−5	nmol/L
34	Ago_d	0	μg
35	Ago_c	0	μg/L = ng/mL
36	$Ago\text{-}R_a$	0	nmol/L
37	$Ago\text{-}R_i$	0	nmol/L
38	Ant_d	0	μg
39	Ant_c	0	μg/L = ng/mL
40	Ant_p	0	μg/L = ng/mL
41	Ant-R	0	nmol/L

or 1000 μg (group 3) Nafarelin daily by intranasal spray. Twenty-seven women completed 6 months of treatment. Inhibition of pituitary-ovarian function by daily intranasal Nafarelin is dose-dependent. In group 1, inhibition of ovulation was inconsistent. Daily doses of 250 or 1000 μg Nafarelin reliably inhibit ovulation, but are associated with reduction of ovarian E2 secretion. Basal serum E2 levels after 1 month of treatment were approximately 70 pg/mL (group 1) and 25 pg/mL (groups 2 and 3). Serum E2 levels increased acutely in response to each dose of Nafarelin in groups 1 and 2, but not in group 3. Thus, average daily E2 levels in group 2 were higher than those in group 3. Basal serum FSH concentrations decreased in all groups. Peak LH responses to Nafarelin decreased by about 70% (groups 1 and 2) and 95% (group 3). After discontinuance of Nafarelin, ovulatory menstrual function returned rapidly in all women.

D.3. Single and multiple dose Cetrorelix data

Citation from Duijkers et al. (1998): This study was conducted as a randomized and single-blind trial. Thirty-six healthy female volunteers (European origin, age between 18 and 35, normal body weight, regular menstrual cycles, functional ovaries) were allocated randomly to three parallel groups of 12 subjects each. One group was treated with 0.25 mg, one with 0.5 mg and the third group with 1.0 mg Cetrorelix acetate salt. Cetrorelix was administered in a first menstrual cycle as a single dose on the individual cycle day 3, and in a second cycle as multiple dose daily between cycle days 3 and 16. For s.c. administration, the amount of Cetrorelix was dissolved in 1 mL water and injected into the lower abdominal wall.

Frequent blood samples were collected for determination of Cetrorelix, FSH, LH, E2 and P4 concentrations. Blood samples for determination of plasma Cetrorelix concentrations were taken in the first treatment cycle on cycle day 3 pre-dose and at 5, 15, 30 min, 1, 1.5, 2, 3, 4, 6, 8, 10, 12, 16, 24, 36, 48, 72, 96 and 120 h post administration. In the second treatment cycle blood samples for Cetrorelix determination were taken on cycle days 3, 9, 13, 14, 15 once pre-dose; on cycle day 16 pre-dose and at 5, 15, 30 min, 1, 1.5, 2, 3, 4, 6, 8, 10, 12, 16, 24, 36, 48, 60, 72, 96, 120, 144 and 168 h post administration.

In the first treatment cycle, blood samples for determination of serum LH, FSH, E2 and P4 concentrations were taken every other day from cycle day 1 until the next menstruation, on cycle day 3 pre-dose, 2, 6 and 12 h post administration, and daily on cycle days 4–9. In the second treatment cycle, samples were taken on alternate days from cycle day 1 until the next menstruation, and on cycle days 3–23 daily. In the post-treatment cycle, E2 and P4 concentrations were measured once between cycle days 1 and 24, to assure ovulation.

A dose-dependent suppression of FSH, LH and E2 concentrations was observed during treatment. After single Cetrorelix administration, median LH, FSH, E2 and P4 concentrations decreased immediately after dosing, but the administration did not result in an apparent delay of ovulation in comparison with the post-treatment cycle. During multiple Cetrorelix treatment, none of the subjects in the 0.5 and 1.0 mg groups had an LH surge or ovulated, whereas the 0.25 mg dose did not completely suppress gonadotropin and steroid activity in all subjects. After multiple administration, ovulation was delayed for 5, 10 and 13 days in the 0.25, 0.5 and 1.0 mg dose groups, respectively. In all groups, median LH, FSH and E2 concentrations increased immediately after cessation of Cetrorelix administration.

D.4. Single dose Cetrorelix data

Citation from Leroy et al. (1994): The study was performed with 10 healthy women (age between 22 and 44, regular ovulatory menstrual cycles of length 26–32 days). A single 5 mg (group 1, 7 women) or 3 mg (group 2, 3 women) dose of Cetrorelix was administered s.c. during the late follicular phase, on the day of cycle when plasma E2 exceeded 150 pg/mL. E2, LH, and P4 levels were measured daily from day 5 of the cycle until day 10 after antagonist treatment. The LH surge was interrupted

in every case. In 6 of 7 subjects from group 1, the LH surge was delayed, occurring 6–17 days after the antagonist injection. In the remaining women, Cetrorelix was administered at the beginning of the LH surge; the LH level fell immediately and the surge was postponed by 3 days. In group 2, in all three subjects the LH surge was delayed, occurring 6–9 days after the injection.

References

Bérault, A., JansemdeAlmeidaCatanho, M.-T., Théoleyre, M., Jutisz, M., 1983. Gonadotropin releasing hormone receptors and the response of pituitary gonadotrophs in culture. J. Endocrinol. 98, 391–399.

Bertram, R., Li, Yue-Xian, 2008. A mathematical model for the actions of activin, inhibin, and follistatin on pituitary gonadotrophs. Bull. Math. Biol. 70, 2211–2228.

Bliss, S.P., Navratil, A.M., Xie, J., Roberson, M.S., 2010. GnRH signaling, the gonadotrope and endocrine control of fertility. Front. Neuroendocrinol. 31, 322–340.

Blum, J.J., Reed, M.C., Janovick, J.A., Conn, P.M., 2000. A mathematical model quantifying GnRH-induced LH secretion from gonadotropes. Am. J. Physiol. Endocrinol. Metab. 278, E263–E272.

Bourne, D.W.A., 1995. Mathematical Modeling of Pharmacokinetic Data. Taylor and Francis, Inc..

Bramley, T.A., Menzies, G.S., 1986. Subcellular fractionation of the human corpus luteum: distribution of GnRH agonist binding sites. Mol. Cell. Endocrinol. 45 (1), 27–36.

Brown, D., Herribson, A.E., Robinson, J.E., Marrs, R.W., Leng, G., 1994. Modelling the luteinizing hormone-releasing hormone pulse generator. Neuroscience 63 (3), 869–879.

Chabbert-Buffet, N., Bouchard, P., 2002. The normal human menstrual cycle. Rev. Endocr. Metab. Disord. 3, 173–183.

Christen, C.A., Moenter, S.M., 2010. The neurobiology of preovulatory and estradiol-induced gonadotropin-releasing hormone surges. Endocr. Rev. 31 (4), 544–577.

Clément, F., Monniaux, D., Stark, J., Hardy, K., Thalabard, J.C., Franks, S., Claude, D., 2001. Mathematical model of FSH-induced cAMP production in ovarian follicles. Am. J. Physiol. Endocrinol. Metab. 281, E35–E53.

Deuflhard, P., 2004. Newton Methods for Nonlinear Problems: Affine Invariance and Adaptive Algorithms. Number 35 in Springer Series in Computational Mathematics. Springer Verlag, Berlin.

Deuflhard, P., Nowak, U., 1986. Efficient numerical simulation and identification of large chemical reaction systems. Ber. Bunsenges. Phys. Chem. 90, 940–946.

Deuflhard, P., Nowak, U., 1987. Extrapolation integrators for quasilinear implicit ODEs. In: Deuflhard, P., Engquist, B. (Eds.), Large Scale Scientific Computing. Birkhäuser, pp. 37–50.

Deuflhard, P., Hairer, E., Zugck, J., 1987. One-step and extrapolation methods for differential-algebraic systems. Numer. Math. 51, 501–516.

Dierkes, T., Wade, M., Nowak, U., Röblitz, S., 2011. BioPARKIN—Biology-Related Parameter Identification in Large Kinetic Networks. ZIB-Report 11-15, Zuse Institute Berlin (ZIB), 2011. 〈http://vs24.kobv.de/opus4-zib/frontdoor/index/index/docId/1270〉.

Duijkers, I.J.M., Klipping, C., Willemsen, W.N.P., Krone, D., Schneider, E., Niebch, G., Hermann, R., 1998. Single and multiple dose pharmacokinetics and pharmacodynamics of the gonadotropin-releasing hormone antagonist Cetrorelix in healthy female volunteers. Hum. Reprod. 13 (9), 2392–2398.

Engel, J.B., Schally, A.V., 2007. Drug insight: clinical use of agonists and antagonists of luteinizing-hormone-releasing hormone. Nat. Clin. Pract. 3 (2), 157–167.

Evans, N.P., Dahl, G.E., Glover, B.H., Karsch, F.J., 1994. Central regulation of pulsatile gonadotropin-releasing hormone (GnRH) secretion by estradiol during the period leading up to the preovulatory GnRH surge in the ewe. Endocrinology 134 (4), 1806. 〈http://endo.endojournals.org/content/134/4/1806.short.

Fauser, B.C., De Jong, D., Olivennes, F., Wramsby, H., Itskovitz-Eldor, J., Tay, C., Van Hooren, H.G., 2002. Endocrine profiles after triggering of final oocyte maturation with GnRH agonist after cotreatment with the GnRH antagonist ganirelix during ovarian hyperstimulation for in vitro fertilization. J. Clin. Endocrinol. Metab. 87 (2), 709–715.

Filicori, M., Flamigni, C., Campaniello, E., Ferrari, P., Meriggioloa, M.C., Michelacci, L., Pareschi, A., Valdiserri, A., 1989. Evidence for a specific role of GnRH pulse frequency in the control of the human menstrual cycle. Am. J. Phys. Endocrinol. Metab. 257 (6), E930–E936.

Filicori, M., Cognigno, G., Dellai, P., Arnone, R., Sambataro, M., Falbo, A., Pecorari, R., Carbone, F., Meriggiola, M.C., 1993. Role of gonadotrophin releasing hormone secretory dynamics in the control of the human menstrual cycle. Hum. Reprod. 8 (2), 62–65.

Garnick, M.B., 2001. History of GnRH antagonists in the management of hormonally responsive disorders a historical overview. Abstract for the Sixth International Symposium on GnRH Analogues in Cancer and Human Reproduction, Geneva, Switzerland, February 2001. 〈http://www.kenes.com/gnrh2001/Abstracts/0112aGarnick.htm〉.

Griesinger, G., Diedrich, K., 2007. GnRH-agonist versus GnRH-antagonist. Frauenarzt 48 (9), 840–844.

Groome, N.P., Illingworth, P.J., O'Brien, M., Pai, R., Rodger, F.E., Mather, J.P., McNeilly, A.S., 1996. Measurement of dimeric inhibin B throughout the human menstrual cycle. J. Clin. Endocrinol. Metab. 81 (4), 1401–1405.

Hall, J.E., 2009. Neuroendocrine control of the menstrual cycle. In: Barbieri Strauss, R.L. (Ed.), Yen and Jaffe's Reproductive Endocrinology: Physiology, Pathophysiology, and Clinical Management, 6 ed. Saunders Elsevier, pp. 139–154. (chapter 7).

Harris, L.A., 2001. Differential Equation Models for the Hormonal Regulation of the Menstrual Cycle. Ph.D. Thesis, North Carolina State University, 2001.

Harris Clark, L., Schlosser, P.M., Selgrade, J.F., 2003. Multiple stable periodic solutions in a model for hormonal control of the menstrual cycle. Bull. Math. Biol. 65, 157–173.

Hayes, F., Hall, J.E., Boepple Jr., P.A., Crowly, W.F., 1998. Differential control of gonadotropin secretion in the human: endocrine role of inhibin. J. Clin. Endocrinol. Metab. 83, 1835–1841.

Heinze, K., Keener, R.W., MidgleyJr, A.R., 1998. A mathematical model of luteinizing hormone release from ovine pituitary cells in perifusion. Am. J. Physiol. Endocrinol. Metab. 275, E1061–E1071.

Herbison, A.E., 1998. Multimodal influence of estrogen upon gonadotropin-releasing hormone neurons. Endocr. Rev. 19 (3), 302.

Jadhav, P.R., Agersø, H., Tornøe, C., Gobburu, J.V.S., 2006. Semi-mechanistic pharmacodynamic modeling for degarelix, a novel gonadotropin releasing hormone (GnRH) blocker. J. Pharmacokinet. Pharmacodyn. 33 (5), 609–634.

Jaffe, R., Monroe, S., Schriock, E., Henzl, M.R., 1986. Inhibition of ovulation by Nafarelin in normal women and women with endometriosis: nasal formulation. ICM Study 1010, Syntex Research, 3401 Hillview Avenue, Palo Alto, California.

Keenan, D.M., Sun, W., Veldhuis, J.D., 2000. A stochastic biomathematical model of the male reproductive hormone system. SIAM J. Appl. Math. 61 (3), 934–965.

Leroy, I., d'Acremont, M.F., Brailly-Tabard, S., Frydman, R., deMouzon, J., Bouchard, P., 1994. A single injection of a gonadotropin-releasing hormone (GnRH) antagonist (Cetrorelix) postpones the luteinizing hormone (LH) surge: further evidence for the role of GnRH during the LH surge. Fertil. Steril. 62 (3), 461–467.

Lim, S., Pnueli, L., Tan, J.H., Naor, Z., Rajagopal, G., Melamed, P., 2009. Negative feedback governs gonadotrope frequency-decoding of gonadotropin releasing hormone pulse-frequency. PLoS ONE 4 (9), 7244.

Loumaye, E., Wynn, P.C., Coy, D., Catt, K.J., 1984. Receptor-binding properties of gonadotropin-releasing hormone derivatives. J. Biol. Chem. 259 (20), 12663.

Macklon, N.S., Fauser, B.C.J.M., 2001. Follicle-stimulating hormone and advanced follicle development in the human. Arch. Med. Res. 31, 595–600.

Magoffin, D.A., Jakimiuk, A.J., 1997. Inhibin A, inhibin B and activin A in the follicular fluid of regularly cycling women. Hum. Reprod. 12 (8), 1714–1719.

Margolskee, A., Selgrade, J.F., 2011. Dynamics and bifurcation of a model for hormonal control of the menstrual cycle with inhibin delay. Math. Biosci. 234 (2), 95–107.

Marshall, J.C., Griffin, M.L., 1993. The role of changing pulse frequency in the regulation of ovulation. Hum. Reprod. 8 (2), 57–61.

McArdle, C.A., Franklin, J., Green, L., Hislop, J.N., 2002. Signalling, cycling and desensitisation of gonadotropin-releasing hormone receptors. J. Endocrinol. 173, 1–11.

McLachlan, R.I., Cohen, N.L., Dahl, K.D., Bremner, W.J., Soules, M.R., 1990. Serum inhibin levels during the periovulatory interval in normal women: Relationships with sex steroid and gonadotrophin levels. Clin. Endocrinol. 32, 39–48.

Metallinou, C., Asimakopoulos, B., Schröer, A., Nikolettos, N., 2007. Gonadotropin-releasing hormone in the ovary. Reprod. Sci. 14, 737–749. 〈http://rsx.sagepub.com/content/14/8/737〉.

Millar, R.P., Lu, Z.-L., Pawson, A.J., Flanagan, C.A., Morgan, K., Maudsley, S.R., 2004. Gonadotropin-releasing hormone receptors. Endocr. Rev. 25 (2), 235–275.

Monroe, S.E., Henzl, M.R., Martin, M.C., Schriock, E., Lewis, V., Nerenberg, C., Jaffe, R.B., 1985. Ablation of folliculogenesis in women by a single dose of gonadotropin-releasing hormone agonist: significance of time in cycle. Fertil. Steril. 43 (8), 361–368.

Monroe, S.E., Blumenfeld, Z., Andreyko, J.L., Schriock, E., Henzl, M.R., Jaffe, R.B., 1986. Dose-dependent inhibition of pituitary-ovarian function during administration of a gonadotropin-releasing hormone agonistic analog (Nafarelin). J. Clin. Endocrinol. Metab. 63 (6), 1334–1341.

Nagaraja, N.V., Pechstein, B., Erb, K., Klipping, C., Hermann, R., Locher, M., Derendorf, H., 2003. Pharamacokinetic/pharamcodynamic modeling of luteinizing hormone (LH) suppression and LH surge delay by Cetrorelix after single and multiple doses in healthy premenopausal women. J. Clin. Pharmacol. 43, 243–251.

Naor, Z., 2009. Signaling by G-protein-coupled receptor (GPCR), studies on the GnRH receptor. Front. Neuroendocrinol. 30, 10–29.

Neill, J.D. (Ed.), 2006. Knobil and Neill's Physiology of Reproduction, 3 ed., vol. 1. Elsevier Academic Press.

Niswender, G.D., Juengel, J.L., Silva, P.J., Rollyson, M.K., McIntush, E.W., 2000. Mechanisms controlling the function and life span of the corpus luteum. Physiol. Rev. 80 (1).

NLSCON, Nonlinear Least Squares Problems with Nonlinear Equality CONstraints. 〈http://www.zib.de/en/numerik/software/codelib/nonlin.html〉.

Nowak, U., Deuflhard, P., 1985. Numerical identification of selected rate constants in large chemical reaction systems. Appl. Numer. Math. 1 (1), 59–75.

Olivennes, F., Ayoubi, J.M., Fanchin, R., Rongieres-Bertrand, C., Hamamah, S., Bouchard, P., Frydman, R., 2000. GnRH antagonist in single-dose applications. Hum. Reprod. Update 6 (4), 313–317.

Pasteur, R.D., 2008. A Multiple-Inhibin Model of the Human Menstrual Cycle. Ph.D. Thesis, North Carolina State University.
Ramaswamy, S., Pohl, C.R., McNeilly, A.S., Winters, S.J., Plant, T.M., 1998. The time course of follicle-stimulating hormone suppression by recombinant human inhibin a in the adult male rhesus monkey. Endocrinology 139 (8), 3409.
Reinecke, I., 2009. Mathematical Modeling and Simulation of the Female Menstrual Cycle. Ph.D. Thesis, Freie Universität Berlin, 2009.
Reinecke, I., Deuflhard, P., 2007. A complex mathematical model of the human menstrual cycle. J. Theor. Biol. 247, 303–330.
Riccobene, T.A., Omann, G.M., Lindermann, J.J., 1999. Modeling activation and desensitization of G-protein coupled receptors provides insight into ligand efficacy. J. Theor. Biol. 200 (2), 207–222.
Schlosser, P.M., Selgrade, J.F., 2000. A model of gonadotropin regulation during the menstrual cycle in women: qualitative features. Environ. Health Perspect. 108 (5), 873–881.
Sehested, A., Juul, A., Andersson, A.M., Petersen, J.H., Jensen, T.K., Müller, J., Skakkebaek, N.E., 2000. Serum inhibin A and inhibin B in healthy prepubertal, pubertal, and adolescent girls and adult women: Relation to age, stage of puberty, menstrual cycle, follicle-stimulating hormone, luteinizing hormone, and estradiol levels. J. Clin. Endocrinol. Metab. 85 (4), 1634–1640.
Selgrade, J.F., 2001. Modeling hormonal control of the menstrual cycle. Comments Theor. Biol. 6 (1), 79–101.
Selgrade, J.F., Schlosser, P.M., 1999. A model for the production of ovarian hormones during the menstrual cycle. Fields Inst. Commun. 21, 429–446.
Shankaran, H., Wiley, H.S., Resat, H., 2007. Receptor downregulation and desensitization enhance the information processing ability of signalling receptors. BMC Syst. Biol. 1, 48.
Strauss III, J.F., 1999. The synthesis and metabolism of steroid hormones. In: Yen, S.S.C., Jaffe, R.B., Barbieri, R.L. (Eds.), Reproductive Endocrinology: Physiology, Pathophysiology, and Clinical Management, 4th ed. W.B. Saunders Company, pp. 125–154.
Strauss III, J.F., 2009. The synthesis and metabolism of steroid hormones. In: Strauss, J.F., Barbieri, R.L. (Eds.), Yen and Jaffe's Reproductive Endocrinology: Physiology, Pathophysiology, and Clinical Management, 6th ed. Saunders Elsevier. (chapter 4).
Struthers, R.S., Xie, Qui, Sullivan, S.K., Reinhart, G.J., Kohout, T.A., Zhu, Yun-Fei, Chen, Chen, Liu, Xin-Jun, Ling, N., Yang, Weidong, Maki, R.A., Bonneville, A.K., Chen, Ta-Kung, Bozigian, H.P., 2007. Pharmacological characterization of a novel nonpeptide antagonist of the human gonadotropin-releasing hormone receptor NBI-42902. Endocrinology 148, 857–867.
Sullivan, S.K., Hoare, S.R.J., Fleck, B.A., Zhu, Yun-Fei, Heise, C.E., Struthers, R.S., Crowe, P.D., 2006. Kinetics of nonpeptide antagonist binding to the human gonadotropin-releasing receptor: implications for structure–activity relationships and insurmountable antagonism. Biochem. Pharmacol. 72, 838–849.
Swerdloff, R.S., Jacobs, H.S., Odell, W.D., 1972. Synergistic role of progestogens in estrogen induction of LH and FSH surge. Endocrinology 90 (6), 1529–1536.
Tavaniotou, A., Smitz, J., Bourgain, C., Devroey, P., 2001. Ovulation induction disrupts luteal phase function. Ann. N.Y. Acad. Sci. 943, 55–63.
Tornøe, C.W., Agersø, H., Senderovitz, T., Nielsen, H.A., Madsen, H., Karlsson, M.O., Jonsson, E.N., 2006. Population pharmacokinetic/pharmacodynamic (PK/PD) modelling of the hypothalamic–pituitary–gonadal axis following treatment with GnRH analogues. Br. J. Clin. Pharmacol. 63 (6), 648–664.
Tsaneva-Atanasova1, K., Mina, P., Caunt, C.J., Armstrong, S.P., McArdle, C.A., 2012. Decoding GnRH neurohormone pulse frequency by convergent signalling modules. J. R. Soc. Interface 9 (66), 170–182.
van der Graaf, P.H., Editorial. 2012. CPT: Pharmacometrics and Systems Pharmacology, 1.
vanLoenen, A.C.D., Huirne, J.A.F., Schats, R., Hompes, P.G.A., Lambalk, C.B., 2002. GnRH agonists, antagonists, and assisted conception. Semin. Reprod. Med. 20 (4), 349–364.
Vidal, A., Clément, F., 2010. A dynamical model for the control of the gonadotropin-releasing hormone neurosecretory system. J. Neuroendocrinol. 22, 1251–1266.
Ward, R. (Ed.), 2011. Quantitative and Systems Pharmacology in the Post-genomic Era: New Approaches to Discovering Drugs and Understanding Therapeutic Mechanisms, QSP White Paper. Quantitative and Systems Pharmacology (QSP) Workshop Group, NIH.
Welt, C.K., McNicholl, D.J., Taylor, A.E., Hall, J.E., 1999. Female reproductive aging is marked by decreased secretion of dimeric inhibin. J. Clin. Endocrinol. Metab. 84, 105–111.
Zeleznik, A.J., 2004. The physiology of follicle selection. Reprod. Biol. Endocrinol. 2 (31).
Zeleznik, A.J., Pohl, C.R., 2006. Control of follicular development, corpus luteum function, the maternal recognition of pregnancy, and the neuroendocrine regulation of the menstrual cycle in higher primates. In: Neill, J.D. (Ed.), Knobil and Neill's Physiology of Reproduction, 3rd ed., vol. 2, chapter 45, Elsevier, pp. 2449–2510.
Zhao, S., Saito, H., Wang, X., Kaneko, T., Hiroi, M., 2000. Effects of gonadotropin-releasing hormone agonist on the incidence of apoptosis in porcine and human granulosa cells. Gynecol. Obstet. Invest. 49, 52–56.